Robotica (2019) volume 37, pp. 1240–1266. © Cambridge University Press 2018
doi:10.1017/S0263574718000826

Kinematic analysis of the 3-RPS-3-SPR series–parallel manipulator

Abhilash Nayak†, Stéphane Caro‡* and Philippe Wenger‡

†*École Centrale de Nantes, Laboratoire des Sciences du Numérique de Nantes (LS2N), Nantes, France*
‡*Centre National de Recherche Scientifique (CNRS), Laboratoire des Sciences du Numérique de Nantes (LS2N), Nantes, France, UMR CNRS 6004*
Emails: stephane.caro@ls2n.fr, philippe.wenger@ls2n.fr

(Accepted August 4, 2018)

SUMMARY
This paper deals with the kinematic analysis and enumeration of singularities of the six degree-of-freedom 3-RPS-3-SPR series–parallel manipulator (S–PM). The characteristic tetrahedron of the S–PM is established, whose degeneracy is bijectively mapped to the serial singularities of the S–PM. Study parametrization is used to determine six independent parameters that characterize the S–PM and the direct kinematics problem is solved by mapping the transformation matrix between the base and the end-effector to a point in $\mathbb{P}^7$. The inverse kinematics problem of the 3-RPS-3-SPR S–PM amounts to find the location of three points on three lines. This problem leads to a minimal octic univariate polynomial with four quadratic factors.

KEYWORDS: Series–parallel Manipualtors; S–PM; Singularities; Characteristic tetrahedron; Inverse kinematics; Direct kinematics.

1. Introduction

Serial and parallel manipulators (SM and PM) have received a lot of interest for the last few decades due to the high stiffness properties of parallel manipulators[1] and large workspace of serial manipulators.[2] Hence, a marriage between SM and PM with a hope to reap the merits of both, has led to hybrid manipulators.[3–9] A hybrid manipulator is a serial linkage mounted on a parallel manipulator and vice-versa or a serial arrangement of two or more parallel manipulators, known as a series–parallel manipulator (S–PM). As much as it is regarded for its merits, an S–PM also bears the demerits of its constituent manipulators in the sense that its kinematic modeling and singularity analysis are more complicated. Various approaches have been proposed in the literature to analyze S–PMs: Shahinpoor[5] solved the direct and inverse kinematics of modular three-axis parallel manipulators mounted in series as an *n*-axis S–PM. Romdhane[8] performed the forward displacement analysis of a Stewart-like S–PM. Tanev[3] studied a novel six degrees-of-freedom (*dof*) S–PM and derived the closed-form solutions to its forward and inverse kinematics. Moreover, Zheng *et al.*[9] obtained closed-form kinematic solutions for the design of a six-*dof* S–PM composed of a three-UPU translational PM and a three-UPU rotational PM mounted in series. In most of these S–PMs, the constituent modules possess the dof that are pure rotations or translations. Hence, each module can be replaced by a set of equivalent lower kinematic pairs that can simplify the understanding of the S–PM behaviour.

There exist other S–PMs in which the PMs that constitute them have their dof coupled and hence give rise to parasitic motions. Hu, Lu and Alvarado[10–12,14,15] have contributed considerably to the design and analysis of this kind of S–PM. Lu and Hu[11] pursued the kinematic analysis of a 2(SP+SPR+SPU) S–PM and plotted its workspace. They also performed the static analysis[10] of S–PMs with *k*-PMs in

* Corresponding author. E-mail: stephane.caro@ls2n.fr

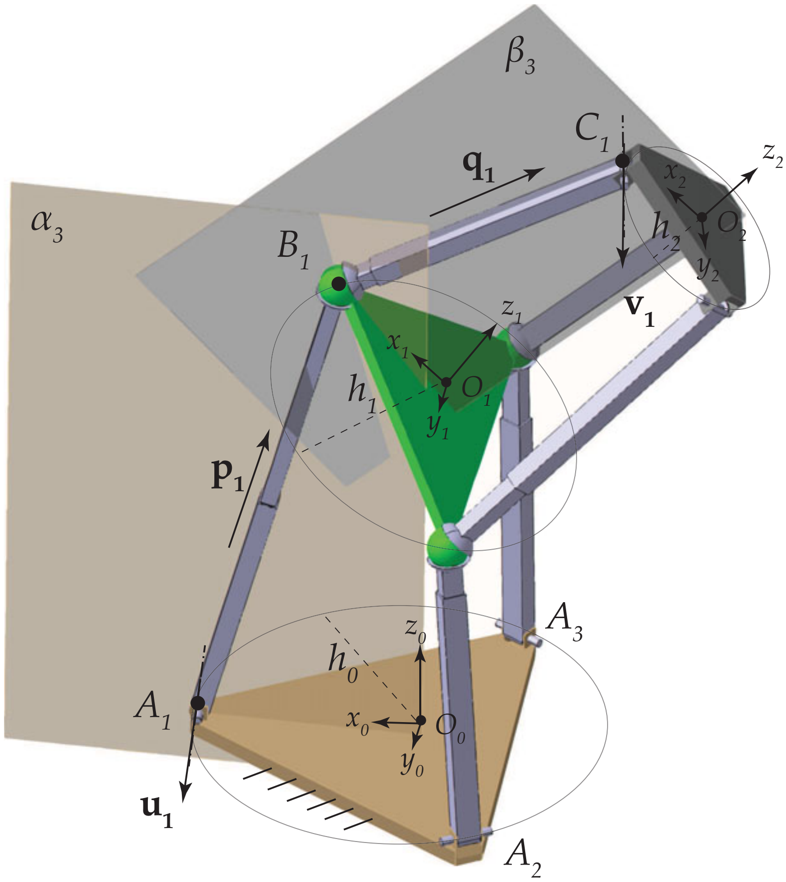

Fig. 1. A 3-RPS-3-SPR series–parallel manipulator.

series. In addition, Hu[14] formulated the Jacobian matrix for S–PMs as a function of Jacobians of the individual parallel modules. Alvarado[12] used screw theory and the principle of virtual work to carry out the kinematic and dynamic analysis of a 2-(3-RPS) S–PM. The 3-RPS-3-SPR S–PM is another example of an S–PM composed of two parallel modules with coupled dof. The proximal module is the three-RPS parallel mechanism which performs a translation and two non-pure rotations about non-fixed axes, which induce two translational parasitic motions,[16] while the distal module is the three-SPR PM that has the same type of *dof*.[24] Hu *et al.*[13] analyzed the workspace of this manipulator. Alvarado *et al.*[15] erroneously claimed that this S–PM has five *dof*. The reader is referred to as Nayak *et al.*[17] for a better understanding of the mobility of this S–PM. Nayak *et al.*[17] proved that the full-cycle mobility of this manipulator is equal to six. Nonetheless, there is very little research on the singularities of S–PMs. It is known that if any of the parallel modules are in a singular configuration, the S–PM is also singular[3] but the singularities that arise due to the serial arrangement of the PMs are generally left out. This paper focuses on the enumeration of those serial singularities in the 3-RPS-3-SPR S–PM. It is shown that six independent parameters can be used to describe the kinematics of this manipulator. Furthermore, direct and inverse kinematics problems for the 3-RPS-3-SPR S–PM are solved using study parametrization.

The paper is organized as follows: The manipulator under study is described in Section 2. Six independent parameters that characterize the S–PM are determined in Section 3. Section 4 presents the singularities of the S–PM, while pointing out its serial singular configurations. Sections 5 and 6 deal with the direct and inverse kinematics problems of the 3-RPS-3-SPR S–PM.

2. Architecture of the 3-RPS-3-SPR Series–Parallel Manipulator

The architecture of the 3-RPS-3-SPR S–PM under study is shown in Fig. 1. It consists of a proximal three-RPS PM module and a distal three-SPR PM module. The three-RPS PM is composed of three legs each containing a revolute, a prismatic and a spherical joint mounted in series, while the legs of the three-SPR PM have these lower pairs in reverse order. Thus, the three equilateral triangular shaped platforms are the fixed base, the coupler and the end effector, coloured brown, green and grey, respectively. The vertices of these platforms are named A_i, B_i and C_i, $i = 1, 2, 3$, respectively. Hereafter, the subscript 0 corresponds to the fixed base, 1 to the coupler platform and 2 to the end-effector. A coordinate frame $\mathcal{F}_i$ is attached to each platform such that its origin O_i lies at its circumcentre. The coordinate axes, x_i points towards the vertex P_1, $P = A, B, C$ y_i is parallel to the opposite side P_3P_2 and by the right-hand rule, z_i is normal to platform plane. Besides, the circum-radius of the ith platform is denoted as h_i. $\mathbf{p}_i$ and $\mathbf{q}_i$, $i = 1, \ldots, 6$ are unit vectors along the prismatic joints, while $\mathbf{u}_i$ and $\mathbf{v}_i$, $i = 1, \ldots, 6$ are unit vectors along the revolute joint axes. α_i is the plane passing through A_i with its normal along $\mathbf{u}_i$. Similarly, β_i is the plane passing through C_i with its normal along $\mathbf{v}_i$. The spherical joint centre B_i is constrained to lie in planes α_i and β_i simultaneously.

3. Parametric Representation of the 3-RPS-3-SPR Series–Parallel Manipulator

This section describes the parametrization of the 3-RPS-3-SPR S–PM shown in Fig. 1. It will be shown that six independent parameters are sufficient to describe the position and orientation of the moving platform. These parameters are obtained by individually parameterizing the proximal and the distal modules.

Study's kinematic mapping[18] maps each spatial Euclidean displacement γ of SE(3) onto a point in seven-dimensional projective space, $\mathbf{p} \in \mathbb{P}^7$. In this parametrization, a point $[x, y, z]$ is transformed to $[x', y', z']$ according to

$$[1, x', y', z']^T = \mathbf{M}[1, x, y, z]^T \tag{1}$$

where the matrix $\mathbf{M} \in SE(3)$ is represented as

$$\mathbf{M} = \begin{bmatrix} {x_0}^2 + {x_1}^2 + {x_2}^2 + {x_3}^2 & \mathbf{0}_{3\times1}^T \\ \mathbf{M}_T & \mathbf{M}_R \end{bmatrix} \tag{2}$$

$$\mathbf{M}_T = \begin{bmatrix} -2x_0y_1 + 2x_1y_0 - 2x_2y_3 + 2x_3y_2 \\ -2x_0y_2 + 2x_1y_3 + 2x_2y_0 - 2x_3y_1 \\ -2x_0y_3 - 2x_1y_2 + 2x_2y_1 + 2x_3y_0 \end{bmatrix} \tag{3}$$

$$\mathbf{M}_R = \begin{bmatrix} {x_0}^2 + {x_1}^2 - {x_2}^2 - {x_3}^2 & -2\,x_0x_3 + 2\,x_1x_2 & 2\,x_0x_2 + 2\,x_1x_3 \\ 2\,x_0x_3 + 2\,x_1x_2 & {x_0}^2 - {x_1}^2 + {x_2}^2 - {x_3}^2 & -2\,x_0x_1 + 2\,x_3x_2 \\ -2\,x_0x_2 + 2\,x_1x_3 & 2\,x_0x_1 + 2\,x_3x_2 & {x_0}^2 - {x_1}^2 - {x_2}^2 + {x_3}^2 \end{bmatrix} \tag{4}$$

where $\mathbf{M}_T$ and $\mathbf{M}_R$ represent the translational and rotational parts of the transformation matrix $\mathbf{M}$, respectively. The parameters $x_i, y_i,\ i \in \{0, \ldots, 3\}$ present in the transformation matrix $\mathbf{M}$ are called the *Study parameters*. An Euclidean transformation can be represented by a point $\mathbf{p} \in \mathbb{P}^7$ if and only if the following equation and inequality are satisfied:

$$x_0y_0 + x_1y_1 + x_2y_2 + x_3y_3 = 0 \tag{5}$$

$${x_0}^2 + {x_1}^2 + {x_2}^2 + {x_3}^2 \neq 0 \tag{6}$$

All the points that satisfy the Eq. (5) belong to the six-dimensional *study quadric*, S_6^2. To avoid the inequality (6), usually a normalization condition $x_i = 1$, $i = 0, 1, 2$ or 3 or $x_0^2 + x_1^2 + x_2^2 + x_3^2 = 1$ is used.

A geometric constraint for each leg of the three-RPS parallel manipulator is that the spherical joint centre is restricted to move in the plane whose normal is directed along the revolute joint axis. Let $f_0, f_1, f_2, f_3, g_0, g_1, g_2, g_3$ be the study parameters. Using study's kinematic mapping,[18,19] three plane constraint equations $E_i = 0$, $i = 1, 2, 3$ can be written as a function of study parameters f_i, g_i, $i = 0, 1, 2, 3$. Along with the study's quadric E_4, there are four constraint equations irrespective of the actuation scheme:

$$E_1 := f_0 f_3 = 0 \tag{7}$$

$$E_2 := {f_1}^2 h_1 - h_1 {f_2}^2 + 2\, f_0 g_1 - 2\, f_1 g_0 - 2\, f_3 g_2 + 2\, g_3 f_2 = 0 \tag{8}$$

$$E_3 := -2\, f_0 f_3 h_1 + f_1 f_2 h_1 - f_0 g_2 + f_1 g_3 + f_2 g_0 - f_3 g_1 = 0 \tag{9}$$

$$E_4 := f_0 g_0 + f_1 g_1 + f_2 g_2 + f_3 g_3 = 0 \tag{10}$$

where h_1 is the circum-radius of the coupler platform. A different set of study parameters, $[c_0, c_1, c_2, c_3, d_0, d_1, d_2, d_3]$ are considered to parameterize the distal module to distinguish the two modules. The constraint equations for the three-SPR PM can be obtained by considering the conjugate of the dual quaternion of the three-RPS PM.[20] In other words, assigning

$$f_0 = c_0, f_1 = -c_1, f_2 = -c_2, f_3 = -c_3, g_0 = d_0, g_1 = -d_1, g_2 = -d_2, g_3 = -d_3 \tag{11}$$

in Eqs. (7) to (10) yields the necessary equations.

Each module is a three *dof* parallel manipulator and to express these mobilities in terms of three parameters, the mechanism should be considered in one of its operation modes (OM). For example, for the three-RPS module, $f_3 = 0$ represents one of its two OM.[21] In this OM, f_0 can never be zero. This fact can be exploited to avoid any point $[f_0, f_1, f_2, f_3, g_0, g_1, g_2, g_3]$ of $\mathbb{P}^7$ to lie on the exceptional generator $f_0 = f_1 = f_2 = f_3 = 0$. This is done by using the normalizing condition, $f_0 = 1$. By substituting $f_3 = 0$ and $f_0 = 1$ in Eqs. (8) to (10), g_0, g_2 and g_3 can be linearly solved as follows:

$$g_0 = 1/2 \frac{f_1 h_1 \left({f_1}^2 - 3\, {f_2}^2\right)}{{f_1}^2 + {f_2}^2 + 1} \tag{12}$$

$$g_2 = -1/2 \frac{f_1 \left(2\, {f_1}^2 g_1 + {f_1}^2 h_1 + 2\, {f_2}^2 g_1 - 3\, {f_2}^2 h_1 + 2\, g_1\right)}{f_2 \left({f_1}^2 + {f_2}^2 + 1\right)} \tag{13}$$

$$g_3 = -1/2 \frac{3\, {f_1}^2 {f_2}^2 h_1 - {f_2}^4 h_1 + 2\, {f_1}^2 g_1 + {f_1}^2 h_1 + 2\, {f_2}^2 g_1 - {f_2}^2 h_1 + 2\, g_1}{f_2 \left({f_1}^2 + {f_2}^2 + 1\right)} \tag{14}$$

Thus, the Euclidean transformation matrix for the proximal module in its OM $f_3 = 0$ can be written as a function of only three parameters f_1, f_2 and g_1:

$$\mathbf{T}_1 = \begin{bmatrix} 1 & 0 & 0 & 0 \\ \dfrac{h_1 \left({f_1}^2 - {f_2}^2\right)}{{f_1}^2 + {f_2}^2 + 1} & \dfrac{{f_1}^2 - {f_2}^2 + 1}{{f_1}^2 + {f_2}^2 + 1} & \dfrac{2 f_1 f_2}{{f_1}^2 + {f_2}^2 + 1} & \dfrac{2 f_2}{{f_1}^2 + {f_2}^2 + 1} \\ -\dfrac{2 h_1 f_2 f_1}{{f_1}^2 + {f_2}^2 + 1} & \dfrac{2 f_1 f_2}{{f_1}^2 + {f_2}^2 + 1} & -\dfrac{{f_1}^2 - {f_2}^2 - 1}{{f_1}^2 + {f_2}^2 + 1} & -\dfrac{2 f_1}{{f_1}^2 + {f_2}^2 + 1} \\ \dfrac{2 {f_1}^2 g_1 + {f_1}^2 h_1 + 2 {f_2}^2 g_1 - {f_2}^2 h_1 + 2\, g_1}{f_2 \left({f_1}^2 + {f_2}^2 + 1\right)} & -\dfrac{2 f_2}{{f_1}^2 + {f_2}^2 + 1} & \dfrac{2 f_1}{{f_1}^2 + {f_2}^2 + 1} & -\dfrac{{f_1}^2 + {f_2}^2 - 1}{{f_1}^2 + {f_2}^2 + 1} \end{bmatrix} \tag{15}$$

Similarly, for the distal three-SPR module in its OM corresponding to $c_3 = 0$, normalizing $c_0 = 1$ and eliminating d_0, d_2 and d_3, the transformation matrix can be derived

https://doi.org/10.1017/S0263574718000826 Published online by Cambridge University Press

as follows:

$$\mathbf{T}_2 = \begin{bmatrix} 1 & 0 & 0 & 0 \\ -\dfrac{c_1{}^4 h_1 - 6\,c_1{}^2 c_2{}^2 h_1 + c_2{}^4 h_1 + 4\,c_1{}^2 d_1 - c_1{}^2 h_1 + 4\,c_2{}^2 d_1 + c_2{}^2 h_1 + 4\,d_1}{\left(c_1{}^2 + c_2{}^2 + 1\right)^2} & \dfrac{c_1{}^2 - c_2{}^2 + 1}{c_1{}^2 + c_2{}^2 + 1} & \dfrac{2c_1 c_2}{c_1{}^2 + c_2{}^2 + 1} & \dfrac{2c_2}{c_1{}^2 + c_2{}^2 + 1} \\ -\dfrac{2c_1(2\,c_1{}^2 c_2{}^2 h_1 - 2\,c_2{}^4 h_1 - 2\,c_1{}^2 d_1 + c_1{}^2 h_1 - 2\,c_2{}^2 d_1 - 2\,c_2{}^2 h_1 - 2\,d_1)}{\left(c_1{}^2 + c_2{}^2 + 1\right)^2 c_2} & \dfrac{2c_1 c_2}{c_1{}^2 + c_2{}^2 + 1} & -\dfrac{c_1{}^2 - c_2{}^2 - 1}{c_1{}^2 + c_2{}^2 + 1} & -\dfrac{2c_1}{c_1{}^2 + c_2{}^2 + 1} \\ \dfrac{2\,c_1{}^4 d_1 - c_1{}^4 h_1 + 4\,c_1{}^2 c_2{}^2 d_1 + 6\,c_1{}^2 c_2{}^2 h_1 + 2\,c_2{}^4 d_1 - c_2{}^4 h_1 + c_1{}^2 h_1 - c_2{}^2 h_1 - 2\,d_1}{\left(c_1{}^2 + c_2{}^2 + 1\right)^2 c_2} & -\dfrac{2c_2}{c_1{}^2 + c_2{}^2 + 1} & \dfrac{2c_1}{c_1{}^2 + c_2{}^2 + 1} & -\dfrac{c_1{}^2 + c_2{}^2 - 1}{c_1{}^2 + c_2{}^2 + 1} \end{bmatrix} \tag{16}$$

Therefore, a transformation matrix between the base frame $\mathcal{F}_0$ and the moving frame $\mathcal{F}_2$ can be expressed as $\mathbf{T} = \mathbf{T}_1.\mathbf{T}_2$ and is a function of six independent parameters. For instance, when both the modules are in the OM represented by $f_3 = 0$ and $c_3 = 0$, $\mathbf{T}$ is a function of f_1, f_2, g_1, c_1, c_2 and d_1 and as a result, indicates that it is indeed a six *dof* mechanism. All possible configurations of the S–PM with its individual modules in different OM, include the following cases:

$$\begin{aligned} &Case\ \ a.\ c_3 = f_3 = 0 \\ &Case\ \ b.\ c_0 = f_0 = 0 \\ &Case\ \ c.\ c_0 = f_3 = 0 \\ &Case\ \ d.\ c_3 = f_0 = 0 \end{aligned} \tag{17}$$

It will be shown in the subsequent sections how simple it is to adapt the results of *Case* a. to the remaining three cases.

Consequently, matrices $\mathbf{T}_1$, $\mathbf{T}_2$ and $\mathbf{T}$ can be used to express the co-ordinates of all the vectors in one frame, preferably the fixed co-ordinate frame $\mathcal{F}_0$ as follows:

$$\begin{aligned} &{}^0\mathbf{r}_{A_1} = [1,\ h_0,\ 0,\ 0]^T;\quad {}^0\mathbf{r}_{A_2} = [1,\ -\frac{h_0}{2},\ \frac{\sqrt{3}h_0}{2},\ 0]^T;\quad {}^0\mathbf{r}_{A_3} = [1,\ -\frac{h_0}{2},\ -\frac{\sqrt{3}h_0}{2},\ 0]^T \\ &{}^1\mathbf{r}_{B_1} = [1,\ h_1,\ 0,\ 0]^T;\quad {}^1\mathbf{r}_{B_2} = [1,\ -\frac{h_1}{2},\ \frac{\sqrt{3}h_1}{2},\ 0]^T;\quad {}^1\mathbf{r}_{B_3} = [1,\ -\frac{h_1}{2},\ -\frac{\sqrt{3}h_1}{2},\ 0]^T \\ &{}^2\mathbf{r}_{C_1} = [1,\ h_2,\ 0,\ 0]^T;\quad {}^2\mathbf{r}_{C_2} = [1,\ -\frac{h_2}{2},\ \frac{\sqrt{3}h_2}{2},\ 0]^T;\quad {}^2\mathbf{r}_{C_3} = [1,\ -\frac{h_2}{2},\ -\frac{\sqrt{3}h_2}{2},\ 0]^T \\ &{}^0\mathbf{u}_1 == [0,\ 0,\ 1,\ 0]^T;\quad {}^0\mathbf{u}_2 = [1,\ -\frac{\sqrt{3}}{2},\ -\frac{1}{2},\ 0]^T;\quad {}^0\mathbf{u}_3 = [1,\ \frac{\sqrt{3}}{2},\ -\frac{1}{2},\ 0]^T \\ &{}^2\mathbf{v}_1 == [0,\ 0,\ 1,\ 0]^T;\quad {}^2\mathbf{v}_2 = [1,\ -\frac{\sqrt{3}}{2},\ -\frac{1}{2},\ 0]^T;\quad {}^2\mathbf{v}_3 = [1,\ \frac{\sqrt{3}}{2},\ -\frac{1}{2},\ 0]^T \\ &{}^0\mathbf{r}_{B_i} = \mathbf{T_1}\,{}^1\mathbf{r}_{B_i};\quad {}^0\mathbf{r}_{C_i} = \mathbf{T}\,{}^2\mathbf{r}_{C_i};\quad {}^0\mathbf{v}_i = \mathbf{T}\,{}^2\mathbf{v}_i,\quad i = 1, 2, 3. \end{aligned} \tag{18}$$

4. Singularities of the 3-RPS-3-SPR S–PM

It is noticed that the 3-RPS-3-SPR S–PM can reach two kinds of singularities: A parallel singularity in which at least one of its modules is in a parallel singularity or a serial singularity[(1)] which occurs

[(1)]A serial singularity is defined here as a configuration in which the S–PM experiences a loss of degree(s) of freedom or, equivalently, a drop in the order of the twist system.

https://doi.org/10.1017/S0263574718000826 Published online by Cambridge University Press

due to the serial arrangement of the two modules. This section briefs the derivation of the forward and inverse kinematic Jacobian matrices with a hope to find out if a given configuration is singular, at least numerically. It also explains a geometrical approach to determine the singularities in which the characteristic tetrahedron[22] of the S–PM under study can be expressed algebraically. The bijective mapping between the degeneracy of the tetrahedron and serial singularities can then be exploited to enlist all the serial singularities.

4.1. Forward and inverse kinematic Jacobian matrices

If the proximal (P) and distal (D) modules are considered individually, the twist i.e., angular velocity vector of a body and linear velocity vector of a point on the body, of their respective moving platform with respect to their fixed base can be expressed as a function of the actuated joint rates[23] as follows:

$$\mathbf{A}_P\, {}^0\mathbf{t}^P_{1/0} = \mathbf{B}_P \dot{p}_{13} \implies \begin{bmatrix} ({}^0\mathbf{r}_{O_1A_1} \times {}^0\mathbf{p}_1)^T & {}^0\mathbf{p}_1^T \\ ({}^0\mathbf{r}_{O_1B_1} \times {}^0\mathbf{p}_2)^T & {}^0\mathbf{p}_2^T \\ ({}^0\mathbf{r}_{O_1C_1} \times {}^0\mathbf{p}_3)^T & {}^0\mathbf{p}_3^T \\ ({}^0\mathbf{r}_{O_1A_1} \times {}^0\mathbf{u}_1)^T & {}^0\mathbf{u}_1^T \\ ({}^0\mathbf{r}_{O_1B_1} \times {}^0\mathbf{u}_2)^T & {}^0\mathbf{u}_2^T \\ ({}^0\mathbf{r}_{O_1C_1} \times {}^0\mathbf{u}_3)^T & {}^0\mathbf{u}_3^T \end{bmatrix} \begin{bmatrix} {}^0\omega^P_{1/0} \\ {}^0\mathbf{v}^P_{O_1/0} \end{bmatrix} = \begin{bmatrix} \mathbf{I}_{3\times3} \\ \mathbf{0}_{3\times3} \end{bmatrix} \begin{bmatrix} \dot{p}_1 \\ \dot{p}_2 \\ \dot{p}_3 \end{bmatrix} \tag{19}$$

$$\mathbf{A}_D\, {}^1\mathbf{t}^D_{2/1} = \mathbf{B}_D \dot{q}_{13} \implies \begin{bmatrix} ({}^1\mathbf{r}_{O_2A_1} \times {}^1\mathbf{q}_1)^T & {}^1\mathbf{q}_1^T \\ ({}^1\mathbf{r}_{O_2B_1} \times {}^1\mathbf{q}_2)^T & {}^1\mathbf{q}_2^T \\ ({}^1\mathbf{r}_{O_2C_1} \times {}^1\mathbf{q}_3)^T & {}^1\mathbf{q}_3^T \\ ({}^1\mathbf{r}_{O_2A_1} \times {}^1\mathbf{v}_1)^T & {}^1\mathbf{v}_1^T \\ ({}^1\mathbf{r}_{O_2B_1} \times {}^1\mathbf{v}_2)^T & {}^1\mathbf{v}_2^T \\ ({}^1\mathbf{r}_{O_2C_1} \times {}^1\mathbf{v}_3)^T & {}^1\mathbf{v}_3^T \end{bmatrix} \begin{bmatrix} {}^1\omega^D_{2/1} \\ {}^1\mathbf{v}^D_{O_2/1} \end{bmatrix} = \begin{bmatrix} \mathbf{I}_{3\times3} \\ \mathbf{0}_{3\times3} \end{bmatrix} \begin{bmatrix} \dot{q}_1 \\ \dot{q}_2 \\ \dot{q}_3 \end{bmatrix} \tag{20}$$

where ${}^0\mathbf{t}^P_{1/0}$ is the twist of the coupler with respect to the base expressed in $\mathcal{F}_0$ and ${}^1\mathbf{t}^D_{2/1}$ is the twist of the end effector with respect to the coupler expressed in $\mathcal{F}_1$. $\mathbf{A}_P$ and $\mathbf{A}_D$ are called forward Jacobian matrices and they incorporate the actuation and constraint wrenches of the three-RPS and three-SPR PMs, respectively.[23] $\mathbf{B}_P$ and $\mathbf{B}_D$ are called inverse Jacobian matrices and they are the result of the reciprocal product between wrenches of the mechanism and twists of the joints for the three-RPS and three-SPR PMs, respectively. $\dot{p}_{13} = [\dot{p}_1, \dot{p}_2, \dot{p}_3]^T$ and $\dot{q}_{13} = [\dot{q}_1, \dot{q}_2, \dot{q}_3]^T$ are the prismatic joint rates of the proximal and distal modules, respectively. ${}^k\mathbf{r}_{PQ}$ denotes the vector pointing from a point P to point Q expressed in frame $\mathcal{F}_k$.

It is noteworthy that if matrix $\mathbf{A}_P$ (resp. $\mathbf{A}_D$) is singular, then the proximal (resp. distal) module will be in a parallel singular configuration. The entries of matrices $\mathbf{A}_P$ and $\mathbf{A}_D$ represent the Plücker coordinates of six independent lines in $\mathbb{P}^3$. When any two or more of these lines are dependent, the configuration corresponds to a parallel singularity. Many scientific papers deal with this singularity type of both modules.[21,24–30] It is noteworthy that the 3-RPS-3-SPR S–PM is in a parallel singularity if and only if any of its modules is in a parallel singularity as proved in the following subsection.

On the other hand, due to the serial stacking of the three-RPS and three-SPR PMs, the S–PM can also have some serial singular configurations even if the individual modules are non-singular[(2)]. Hence, a kinematic Jacobian matrix of the S–PM is necessary to explore the serial singularities. If both $\mathbf{A}_P$ and $\mathbf{A}_D$ are non-singular, the so-called serial Jacobian matrix of the S–PM can be expressed

[(2)]The three-RPS and the three-SPR PMs do not have any serial singularities as long as the prismatic link lengths p_i and q_i, $i = 1, 2, 3$ do not vanish.

https://doi.org/10.1017/S0263574718000826 Published online by Cambridge University Press

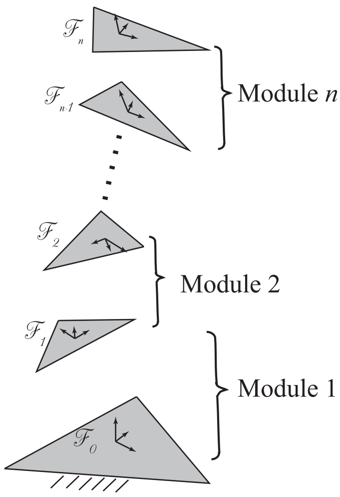

Fig. 2. n parallel mechanisms (named modules) arranged in series.

as follows:[17]

$$\mathbf{J}_{\text{S–PM}} = \left[{}^{2}\mathbf{Ad}_1\, \mathbf{A}_P^{-1}\, \mathbf{B}_P \quad {}^{0}\overline{\mathbf{R}}_1\, \mathbf{A}_D^{-1}\, \mathbf{B}_D \right] \tag{21}$$

$$\text{with} \quad {}^{2}\mathbf{Ad}_1 = \begin{bmatrix} \mathbf{I}_{3\times3} & \mathbf{0}_{3\times3} \\ -{}^{0}\hat{\mathbf{r}}_{O_1O_2} & \mathbf{I}_{3\times3} \end{bmatrix}, \quad {}^{0}\hat{\mathbf{r}}_{O_1O_2} = \begin{bmatrix} 0 & -{}^{0}z_{O_1O_2} & {}^{0}y_{O_1O_2} \\ {}^{0}z_{O_1O_2} & 0 & -{}^{0}x_{O_1O_2} \\ -{}^{0}y_{O_1O_2} & {}^{0}x_{O_1O_2} & 0 \end{bmatrix}$$

$$\text{and} \quad {}^{0}\overline{\mathbf{R}}_1 = \begin{bmatrix} {}^{0}\mathbf{R}_1 & \mathbf{I}_{3\times3} \\ \mathbf{I}_{3\times3} & {}^{0}\mathbf{R}_1 \end{bmatrix}$$

where ${}^{2}\mathbf{Ad}_1$ is called the adjoint matrix. ${}^{0}\hat{\mathbf{r}}_{O_1O_2}$ is the cross product matrix of vector ${}^{0}\mathbf{r}_{O_1O_2} = [{}^{0}x_{O_1O_2}, {}^{0}y_{O_1O_2}, {}^{0}z_{O_1O_2}]$, pointing from point O_1 to point O_2 expressed in frame $\mathcal{F}_0$. ${}^{0}\overline{\mathbf{R}}_1$ is called the augmented rotation matrix between frames $\mathcal{F}_0$ and $\mathcal{F}_1$ and it contains the rotation matrix ${}^{0}\mathbf{R}_1$ from frame $\mathcal{F}_0$ to frame $\mathcal{F}_1$. $\mathbf{J}_{\text{S–PM}}$ fits into the kinematic model of the S–PM in the following way:

$${}^{0}\mathbf{t}_{2/0} = \mathbf{J}_{\text{S–PM}} \begin{bmatrix} \dot{\mathbf{p}} \\ \dot{\mathbf{q}} \end{bmatrix} \tag{22}$$

where ${}^{0}\mathbf{t}_{2/0}$ is the twist of the moving platform with respect to the fixed base expressed in $\mathcal{F}_0$ and $\dot{\mathbf{p}} = [\dot{p}_1, \dot{p}_2, \dot{p}_3]^T$ and $\dot{\mathbf{q}} = [\dot{q}_1, \dot{q}_2, \dot{q}_3]^T$ are the joint rates of the proximal and the distal modules, respectively. The rank of this matrix provides the local mobility of the S–PM.[17] Moreover, when $\mathbf{J}_{\text{S–PM}}$ is singular, the S–PM at hand is in a serial singularity. When a manipulator configuration is given, it is straightforward to calculate numerically the serial kinematic Jacobian matrix from Eq. (21) and to deduce if it is a serial singular configuration. However, it is tedious to derive a symbolic or an implicit equation that could be used to enlist all serial singularities. Therefore, a geometric approach is adopted.

Equations (21) and (22) can be extended to an S–PM with n number of modules in series as shown in Fig. 2. Thus, the moving platform twist with respect to the fixed base expressed in coordinate frame

https://doi.org/10.1017/S0263574718000826 Published online by Cambridge University Press

$\mathcal{F}_0$ is as follows:

$$
\begin{gathered}
{}^0\mathbf{t}_{n/0} = \sum_{i=1}^{n} {}^0\overline{\mathbf{R}}_{(i-1)}\, {}^n\mathbf{Ad}_i\, {}^{(i-1)}\mathbf{t}^{M_i}_{i/(i-1)} = \mathbf{J}_{6\times 3n} \begin{bmatrix} \dot{\rho}_{M_1} \\ \dot{\rho}_{M_2} \\ \vdots \\ \dot{\rho}_{M_n} \end{bmatrix} \\
\text{with } {}^0\overline{\mathbf{R}}_i = \begin{bmatrix} {}^0\mathbf{R}_i & \mathbf{I}_{3\times 3} \\ \mathbf{I}_{3\times 3} & {}^0\mathbf{R}_i \end{bmatrix}, \quad {}^n\mathbf{Ad}_i = \begin{bmatrix} \mathbf{I}_{3\times 3} & \mathbf{0}_{3\times 3} \\ -{}^{(i-1)}\hat{\mathbf{r}}_{O_iO_n} & \mathbf{I}_{3\times 3} \end{bmatrix} \text{ and} \\
\mathbf{J}_{6\times 3n} = \begin{bmatrix} {}^n\mathbf{Ad}_1\, \mathbf{A}^{-1}_{M_0}\mathbf{B}_{M_0} & {}^0\overline{\mathbf{R}}_1\, {}^n\mathbf{Ad}_2 \mathbf{A}^{-1}_{M_1}\mathbf{B}_{M_1} & \dots & {}^0\overline{\mathbf{R}}_n\, \mathbf{A}^{-1}_{M_n}\mathbf{B}_{M_n} \end{bmatrix}
\end{gathered}
\tag{23}
$$

where $\mathbf{J}_{6\times 3n}$ is the $6 \times 3n$ kinematic Jacobian matrix of the n-module S–PM manipulator. M_i stands for the ith module, $\mathbf{A}_{M_i}$ and $\mathbf{B}_{M_i}$ are the forward and inverse Jacobian matrices of M_i, respectively. $\dot{\rho}_{M_i}$ is the vector of the actuated prismatic joint rates for the ith module.

4.2. Twist and wrench systems of the 3-RPS-3-SPR PM

Each leg of the three-RPS and three-SPR parallel manipulators is composed of three joints, but the order of the limb twist system is equal to five and hence there exist five twists associated to each leg. Thus, the constraint wrench system of the ith leg of the three-RPS and three-SPR parallel modules is spanned by a pure force $\mathcal{W}^i_P$ and $\mathcal{W}^i_D$ shown as the black and red vectors, respectively, in Fig. 4. These forces are reciprocal to all the joint twists in each leg, in the respective modules. The three forces in each module span its wrench system $\mathcal{W}_P$ or $\mathcal{W}_D$ which is the *third special three-system* of screws:[16]

$$
\begin{aligned}
{}^0\mathcal{W}_P &= \bigoplus_{i=1}^{3} {}^0\mathcal{W}^i_P = \text{span}\left\{ \begin{bmatrix} {}^0\mathbf{u}_1 \\ {}^0\mathbf{r}_{O_2B_1} \times {}^0\mathbf{u}_1 \end{bmatrix}, \begin{bmatrix} {}^0\mathbf{u}_2 \\ {}^0\mathbf{r}_{O_2B_2} \times {}^0\mathbf{u}_2 \end{bmatrix}, \begin{bmatrix} {}^0\mathbf{u}_3 \\ {}^0\mathbf{r}_{O_2B_3} \times {}^0\mathbf{u}_3 \end{bmatrix} \right\} \\
{}^0\mathcal{W}_D &= \bigoplus_{i=1}^{3} {}^0\mathcal{W}^i_D = \text{span}\left\{ \begin{bmatrix} {}^0\mathbf{v}_1 \\ {}^0\mathbf{r}_{O_2B_1} \times {}^0\mathbf{v}_1 \end{bmatrix}, \begin{bmatrix} {}^0\mathbf{v}_2 \\ {}^0\mathbf{r}_{O_2B_2} \times {}^0\mathbf{v}_2 \end{bmatrix}, \begin{bmatrix} {}^0\mathbf{v}_3 \\ {}^0\mathbf{r}_{O_2B_3} \times {}^0\mathbf{v}_3 \end{bmatrix} \right\} \\
{}^0\mathcal{W}_{S-PM} &= {}^0\mathcal{W}_P \cap {}^0\mathcal{W}_D \\
\dim({}^0\mathcal{W}_P) &= \dim({}^0\mathcal{W}_D) = 3
\end{aligned}
\tag{24}
$$

Alternatively, the twist system of the 3-RPS-3-SPR S–PM is the union of the twist systems of two modules. The twist systems of each module are the orthogonal vector subspaces of the respective wrench systems and are also the *third special three-system* of screws:[16]

$$
\begin{aligned}
{}^0\mathcal{T}_P &= {}^0\mathcal{W}_P^{\perp} \\
{}^0\mathcal{T}_D &= {}^0\mathcal{W}_D^{\perp} \\
{}^0\mathcal{T}_{S-PM} &= {}^0\mathcal{T}_P \cup {}^0\mathcal{T}_D \\
\dim({}^0\mathcal{T}_P) &= \dim({}^0\mathcal{T}_D) = 3
\end{aligned}
\tag{25}
$$

The mobility of the 3-RPS-3-SPR S–PM is equal to the dimension of the overall twist system, $\dim({}^0\mathcal{T}_{S-PM})$. For a general configuration, when the twist systems of each module are independent, i.e., $\dim({}^0\mathcal{T}_P \cap {}^0\mathcal{T}_D) = 0$, the mobility was established to be six in ref. [17]:

$$
\begin{aligned}
\dim({}^0\mathcal{T}_{S-PM}) = \dim({}^0\mathcal{T}_P \cup {}^0\mathcal{T}_D) &= \dim({}^0\mathcal{T}_P) + \dim({}^0\mathcal{T}_D) - \dim({}^0\mathcal{T}_P \cap {}^0\mathcal{T}_D) \\
&= \dim({}^0\mathcal{T}_P) + \dim({}^0\mathcal{T}_D) \\
&= 3 + 3 = 6
\end{aligned}
\tag{26}
$$

As a conclusion, the following theorem is stated.

https://doi.org/10.1017/S0263574718000826 Published online by Cambridge University Press

THEOREM 1. *A parallel singularity of an S–PM arises if and only if at least one of its modules reaches a parallel singularity.*

Proof: When the actuators are blocked, the twist system of any module in a parallel singularity is of order more than zero or, equivalently, the wrench system is of order less than six. The sufficient condition is that if at least one module is in a parallel singularity, then the S–PM is in a parallel singularity. In this case, from Eq. (26), if the order of the twist system is more than zero for any module, it is reflected in the order of the twist system of the whole S–PM. The necessary condition can be proved as follows. If none of the modules is in a parallel singularity, the wrench system of each module is of order six when the actuated joints are blocked. Thus, the order of the wrench system of the full S–PM is also of order six and thus the S–PM is not in a parallel singularity.

4.3. Enumeration of serial singularities

A serial singularity is encountered

- when there exists a wrench common to both the modules of the S–PM or, equivalently, if the dimension of the intersection of the two wrench systems is more than zero:

$$\dim({}^0\mathcal{W}_P \cap {}^0\mathcal{W}_D) > 0 \tag{27}$$

- if the union of the two wrench systems is of dimension lower than six. Indeed,

$$\begin{aligned}\dim({}^0\mathcal{W}_P \cup {}^0\mathcal{W}_D) &= \dim({}^0\mathcal{W}_P) + \dim({}^0\mathcal{W}_D) - \dim({}^0\mathcal{W}_P \cap {}^0\mathcal{W}_D)\\ &= 3 + 3 - \dim({}^0\mathcal{W}_P \cap {}^0\mathcal{W}_D)\end{aligned} \tag{28}$$

  From Eqs. (27) and (28), $\dim({}^0\mathcal{W}_P \cup {}^0\mathcal{W}_D) < 6$.

A straightforward sufficient condition for Eq. (27) or (28) to hold is that at least one revolute joint axis in the base is parallel to the corresponding revolute joint axis in the moving platform. In other words, ${}^0\mathbf{u_i} \,||\, {}^0\mathbf{v_i}$ for any $i = 1, 2, 3$. For the ith leg, by equating the coordinates of vectors ${}^0\mathbf{u_i}$ and ${}^0\mathbf{v_i}$, three systems of equations are obtained from Eq. (18) in parameters c_1, c_2, f_1 and f_2. Solving the system of equations for three of the four parameters, say, c_1, f_1 and c_2 leads to the following algebraic expressions corresponding to the serial singular configurations:

$$\begin{aligned}{}^0\mathbf{u_1} \,||\, {}^0\mathbf{v_1} &\implies c_1 = 0,\ f_1 = 0\\ {}^0\mathbf{u_2} \,||\, {}^0\mathbf{v_2} &\implies c_1 = -\sqrt{3}c_2,\ f_1 = -\sqrt{3}f_2\\ {}^0\mathbf{u_3} \,||\, {}^0\mathbf{v_3} &\implies c_1 = \sqrt{3}c_2,\ f_1 = \sqrt{3}f_2\\ {}^0\mathbf{u_i} \,||\, {}^0\mathbf{v_i} \quad \forall i = 1, 2, 3 &\implies c_1 = -f_1,\ c_2 = -f_2\end{aligned} \tag{29}$$

When all the base revolute joint axes are parallel to their corresponding platform revolute joint axes, the fixed base and the moving platform are parallel to each other. In this case, the transformation matrix $\mathbf{T}$ is the identity matrix resulting in $\mathbf{T}_1 = \mathbf{T}_2^{-1}$. Figure 3 shows the four cases for arbitrary design parameters. In the first three cases, the constraint wrench τ_0 prevents the moving platform from rotating about its axis. Thus, the manipulator has only five *dof*. When the base is parallel to the moving platform, the constraint wrench system of the whole manipulator is spanned by three forces τ_{01}, τ_{02} and τ_{03} leading to an instantaneous three *dof* S–PM. The dofs include a pure vertical translation and two non-pure horizontal rotations. In this case, the last condition shown in (29) can be substituted in the expression for $\mathbf{T}$ to find the coordinates of the platform circumcentre O_2 to be $[0, 0, \frac{2(d_1 + g_1)}{f_2}]$, where only a z-translation is allowed. There can be other similar configurations in which the base and the platform are parallel with translations along all three coordinate axes. It is noteworthy that the algebraic relations governing the serial singular configurations described so far are independent of the parameters h_0, h_1, h_2, g_1 and d_1.

https://doi.org/10.1017/S0263574718000826 Published online by Cambridge University Press

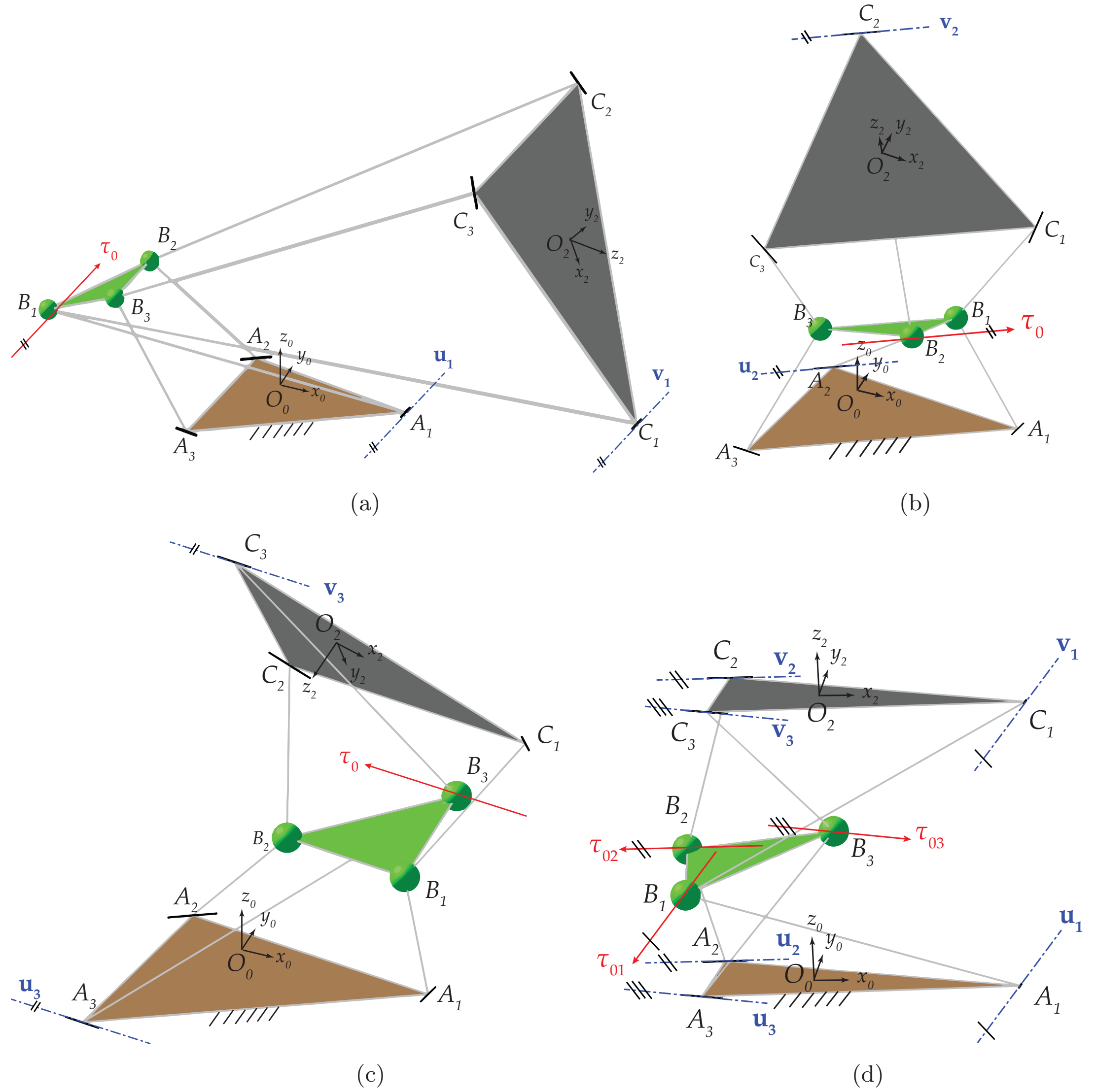

Fig. 3. Serial singular configurations with parallel revolute joint axes. (a) ${}^{0}\mathbf{u_1} \,||\, {}^{0}\mathbf{v_1}$. (b) ${}^{0}\mathbf{u_2} \,||\, {}^{0}\mathbf{v_2}$. (c) ${}^{0}\mathbf{u_3} \,||\, {}^{0}\mathbf{v_3}$. (d) ${}^{0}\mathbf{u_i} \,||\, {}^{0}\mathbf{v_i}\ \forall i = 1, 2, 3$.

There exist other serial singular configurations in which the constraint wrenches at each spherical joint are not coincident and hence form the *first special two system* of screws.[16] The following section describes a methodology to determine these singularities.

4.4. Characteristic tetrahedron of serial singularities

At each spherical joint, if the constraint forces are not coincident, they form a force *pencil*. A *characteristic tetrahedron* is defined combining the planes of the three pencils along with the coupler platform plane passing through the spherical joints as shown in Fig. 4.

A theorem proposed by Uphoff *et al.* in ref. [22] is used to identify the remaining serial singularities.

THEOREM 2 (ref. [22]). *A platform manipulator is in a wrench singularity if and only if the characteristic tetrahedron is singular.*

In this context, the wrench singularities correspond to the serial singularities of the S–PM. The method was initially designed to determine the parallel singularities of a parallel manipulator and the novelty of this paper lies in using the same method to enumerate serial singularities of an S–PM. The homogeneous co-ordinates of the planes (the normal vector to the plane, $\mathbf{w}_i$ and a point on the

https://doi.org/10.1017/S0263574718000826 Published online by Cambridge University Press

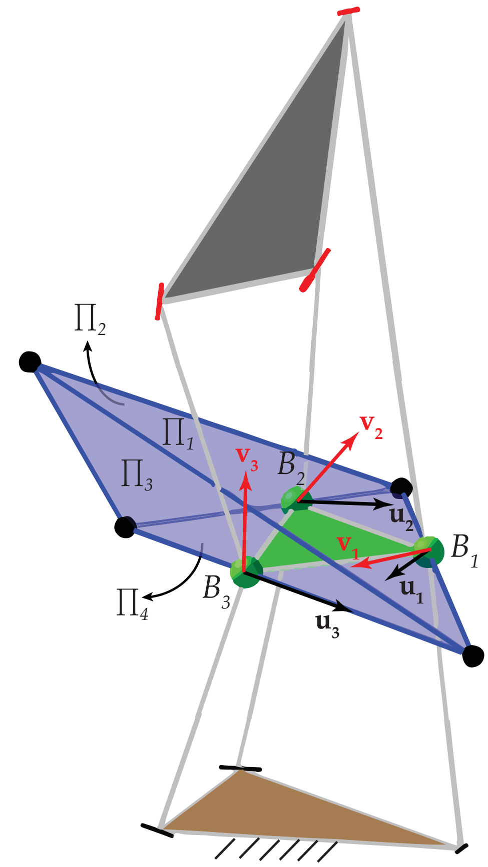

Fig. 4. The characteristic tetrahedron of the 3-RPS-3-SPR S–PM.

plane are known) representing the faces of the tetrahedron are expressed as follows:

$$\begin{aligned}
\Pi_1 &: \mathbf{a} = [w_{01},\ \mathbf{w}_1] = [-\mathbf{r}_{B_1}^T(\mathbf{u}_1 \times \mathbf{v}_1),\quad (\mathbf{u}_1 \times \mathbf{v}_1)^T] \\
\Pi_2 &: \mathbf{b} = [w_{02},\ \mathbf{w}_2] = [-\mathbf{r}_{B_2}^T(\mathbf{u}_2 \times \mathbf{v}_2),\quad (\mathbf{u}_2 \times \mathbf{v}_2)^T] \\
\Pi_3 &: \mathbf{c} = [w_{03},\ \mathbf{w}_3] = [-\mathbf{r}_{B_3}^T(\mathbf{u}_3 \times \mathbf{v}_3),\quad (\mathbf{u}_3 \times \mathbf{v}_3)^T] \\
\Pi_4 &: \mathbf{d} = [w_{04},\ \mathbf{w}_4] \\
&\quad = [-\mathbf{r}_{B_1}^T((\mathbf{r}_{B_1} - \mathbf{r}_{B_2}) \times (\mathbf{r}_{B_1} - \mathbf{r}_{B_3})),\quad ((\mathbf{r}_{B_1} - \mathbf{r}_{B_2}) \times (\mathbf{r}_{B_1} - \mathbf{r}_{B_3}))^T]
\end{aligned} \tag{30}$$

All the vectors are expressed in frame $\mathcal{F}_0$. Hence, a serial singularity occurs when the determinant of the matrix of plane coordinates $[\mathbf{a\,b\,c\,d}]$ vanishes. A similar approach using Grassman–Cayley algebra was used to find singularities of a six-dof manipulator, Three-$\underline{\text{PP}}$PS in ref. [31]. From Eqs. (18) and (30),

$$\begin{aligned}
|\mathbf{a\,b\,c\,d}| = &-\frac{27\,(c_1 f_1 + c_2 f_2 - 1)\,h_1{}^3}{2\left(c_1{}^2 + c_2{}^2 + 1\right)^3 \left(f_1{}^2 + f_2{}^2 + 1\right)^3}(4\,c_1{}^4 f_1 f_2{}^2 - 8\,c_1{}^3 c_2 f_1{}^2 f_2 - 8\,c_1{}^3 c_2 f_2{}^3 \\
&+ 4\,c_1{}^3 f_1{}^2 f_2{}^2 - 4\,c_1{}^3 f_2{}^4 + 4\,c_1{}^2 c_2{}^2 f_1{}^3 + 12\,c_1{}^2 c_2{}^2 f_1 f_2{}^2 - 8\,c_1{}^2 c_2 f_1{}^3 f_2 \\
&+ 4\,c_1 c_2{}^2 f_1{}^4 + 12\,c_1 c_2{}^2 f_1{}^2 f_2{}^2 - 4\,c_2{}^4 f_1{}^3 - 8\,c_2{}^3 f_1{}^3 f_2 + c_1{}^4 f_1 - 8\,c_1{}^3 c_2 f_2 \\
&+ 3\,c_1{}^3 f_1{}^2 - 3\,c_1{}^3 f_2{}^2 + 6\,c_1{}^2 c_2{}^2 f_1 - 6\,c_1{}^2 c_2 f_1 f_2 + 3\,c_1{}^2 f_1{}^3 + 3\,c_1{}^2 f_1 f_2{}^2
\end{aligned}$$

https://doi.org/10.1017/S0263574718000826 Published online by Cambridge University Press

$$+ 3\,c_1c_2^{\,2}f_1^{\,2} - 3\,c_1c_2^{\,2}f_2^{\,2} - 6\,c_1c_2f_1^{\,2}f_2 - 6\,c_1c_2f_2^{\,3} + c_1f_1^{\,4} + 6\,c_1f_1^{\,2}f_2^{\,2}$$
$$- 3\,c_1f_2^{\,4} - 3\,c_2^{\,4}f_1 - 6\,c_2^{\,3}f_1f_2 - 3\,c_2^{\,2}f_1^{\,3} - 3\,c_2^{\,2}f_1f_2^{\,2} - 8\,c_2f_1^{\,3}f_2 + c_1^{\,3}$$
$$+ 3\,c_1^{\,2}f_1 - 3\,c_1c_2^{\,2} - 6\,c_1c_2f_2 + 3\,c_1f_1^{\,2} - 3\,c_1f_2^{\,2} - 3\,c_2^{\,2}f_1 - 6\,c_2f_1f_2$$
$$+ f_1^{\,3} - 3\,f_1f_2^{\,2}) \tag{31}$$

Thus, the points on the surface $|\mathbf{a}\,\mathbf{b}\,\mathbf{c}\,\mathbf{d}| = 0$ correspond to serial singular configurations for the 3-RPS-3-SPR S–PM. From Eq. (31), the manipulator is in a serial singular configuration when either $c_1f_1 + c_2f_2 - 1 = 0$ or the second factor, a 7° polynomial, $p^7(c_1, f_1, c_2, f_2) = 0$[(3)]. In order to enumerate different serial singularities, the conditions for rank deficiency of the matrix $[\mathbf{a}\,\mathbf{b}\,\mathbf{c}\,\mathbf{d}]$ listed in Table 1 of ref. [22] are studied.

Case 1: Four faces meet in a point: Two subcases must be considered depending on whether the point of intersection is real or lies at infinity. In both cases, the variety spanned by the six constraint wrench lines is a *general linear complex*[32] and the 3-RPS-3-SPR S–PM instantaneously behaves as a five *dof* mechanism.

a. A real point: Considering the second factor of Eq. (31) $p^7(c_1, c_2, f_1, f_2)$, substituting arbitrary values for any three of the four parameters and finding the fourth one shows that the faces of the characteristic tetrahedron intersect in a point. One such configuration is shown in Fig. 5a. Point P is the intersection point of the four planes Π_j, $j = 1, 2, 3, 4$.

b. A point at infinity: This happens when the intersection lines of the planes are parallel. In other words, it is sufficient to check if the ideal point (nothing but the point at infinity of a line) of one of these lines lies in the other three planes. Let the ideal point of line of intersection, L_{12}, of planes Π_1 and Π_2 be P_{12}^{∞}. It is sufficient to check if this point lies on the line of intersection, L_{34}, of planes Π_3 and Π_4. However, this approach is computationally expensive and yields no results. Therefore, it is first checked whether point P_{12}^{∞} lies on the line of intersection, L_{13}, of planes Π_1 and Π_3 as follows:

$$\mathbf{r}_{P_{12}^{\infty}} : (0, \mathbf{l}_{12}) = (0, \mathbf{w}_1 \times \mathbf{w}_2) \tag{32}$$

$$L_{13} : (\mathbf{l}_{13},\ \bar{\mathbf{l}}_{13}) = (\mathbf{w}_1 \times \mathbf{w}_3,\ w_{01}\mathbf{w}_3 - w_{03}\mathbf{w}_1) \tag{33}$$

$$\mathbf{r}_{P_{12}^{\infty}}^{\infty} \wedge L_{12} = 0 : \mathbf{w}_3 \cdot \mathbf{l}_{12} = 0, \quad -w_{03}\mathbf{l}_{12} + \mathbf{w}_3 \times \bar{\mathbf{l}}_{12} = 0 \tag{34}$$

Solving Eq. (34) for c_1, f_1, c_2 and f_2 yields the relationship $c_1f_1 + c_2f_2 - 1 = 0$ or $c_1f_2 - c_2f_1 = 0$. The former relationship corresponds to the intersection of the planes in a real line. It will be discussed in the following paragraph. The latter corresponds to the configuration where the planes Π_1, Π_2 and Π_3 share the same ideal point. It can also mean that they have a common line of intersection at infinity, which will be dealt with in the next paragraph. In other words, their lines of intersection are parallel. Formulating another equation such that the point P_{12}^{∞} lies in the plane Π_4 and solving the two equations results in the following relationships:

$$\left.\begin{array}{l} c_1f_2 - c_2f_1 = 0 \\ \mathbf{r}_{P_{12}^{\infty}} \cdot ([w_{04},\ \mathbf{w}_4]) = 0 \end{array}\right\} \Longrightarrow \begin{array}{c} f_1 = -\dfrac{c_1}{c_1^2 + c_2^2},\ f_2 = -\dfrac{c_2}{c_1^2 + c_2^2} \\ \text{OR} \\ c_1 = -\dfrac{f_1}{f_1^2 + f_2^2},\ c_2 = -\dfrac{f_2}{f_1^2 + f_2^2} \end{array} \tag{35}$$

If the parameters c_1, c_2, f_1 and f_2 satisfy the foregoing conditions, the S–PM is in a serial singularity with the planes of its characteristic tetrahedron intersecting in a point at infinity. One such configuration is depicted in Fig. 5b.

[(3)]A 3D animation of the singular surface by varying c_1, c_2, f_1 and f_2 from -3 to 3 is uploaded in https://www.dropbox.com/s/dzif65bhx59nxd6/sing1.mp4?dl=0 for the first factor of Eq. (31) and in https://www.dropbox.com/s/koezrl6xom3pmmr/singp7.mp4?dl=0 for the second factor of Eq. (31).

https://doi.org/10.1017/S0263574718000826 Published online by Cambridge University Press

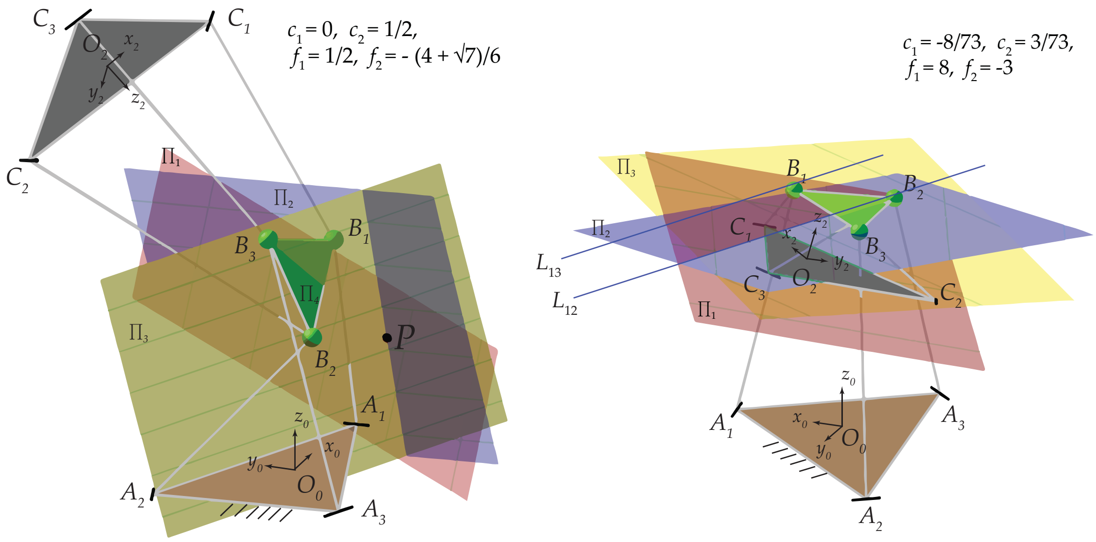

(a) (b)

Fig. 5. Serial singularity when all faces of the characteristic tetrahedron meet in a point. (a) A real point P. (b) A point at infinity.

Case 2: Three sides meet in a line: : The first factor of Eq. (31), $c_1 f_1 + c_2 f_2 - 1 = 0$ corresponds to the serial singularity in which the variety spanned by the six constraint wrench lines is a *special linear complex*[32] and the mechanism has five *dof*. To prove that $c_1 f_1 + c_2 f_2 = 1$ corresponds to the singularity when three sides of the characteristic tetrahedron meet in a line, two subcases are considered when the line of intersection of the three sides is

a. a real line: The condition $c_1 f_1 + c_2 f_2 - 1 = 0$ is derived using line geometry. For a line intersection of the three planes, it is sufficient to prove the incidence of the intersection line of first two sides with the third one. The Plücker coordinates of the line of intersection, L_{12} of planes Π_1 and Π_2 are calculated. The line L_{12} and the plane Π_3 are incident if and only if the following conditions are satisfied:[33]

$$L_{12} : (\mathbf{l}_{12},\ \bar{\mathbf{l}}_{12}) = (\mathbf{w}_1 \times \mathbf{w}_2,\ w_{01}\mathbf{w}_2 - w_{02}\mathbf{w}_1) \tag{36}$$

$$\Pi_3 \wedge L_{12} = 0 : \mathbf{w}_3 \cdot \mathbf{l}_{12} = 0, \quad -w_{03}\mathbf{l}_{12} + \mathbf{w}_3 \times \bar{\mathbf{l}}_{12} = 0 \tag{37}$$

The four equations in Eq. (37) are solved for parameters c_1, c_2, f_1 and f_2 to obtain the solution $f_2 = -\dfrac{c_1 f_1 - 1}{c_2}$ with arbitrary values for c_1, c_2 and f_1. It means that if the choice of these parameters are bound by the relation $c_1 f_1 + c_2 f_2 - 1 = 0$, the three sides intersect in a line and is consistent with the first factor of Eq. (31). Figure 6a shows one of the serial singular configurations in which the three sides meet in a line L. It implies that six constraint forces intersect the line L and hence belong to a singular linear line complex.

b. a line at infinity: In this case, the side planes are all parallel to each other which is possible only when the fixed base and the moving platform planes are parallel to each other. Since the 3-RPS-3-SPR PM has six dof, the only possibilities for the platform and the base to remain parallel is when the moving platform has pure translational motions or has a rotation about the z_0-axis along with translational motions. The former case is studied in Section 4.3, where corresponding revolute joint axes are parallel to each other leading to a three *dof* freedom mechanism. The latter case is investigated by considering the transformation matrix $\mathbf{T}$, and forcing the rotation matrix to be of pure rotation about z_0-axis. This is done by equating $\mathbf{T}(2, 4)$ and $\mathbf{T}(3, 4)$ to zero and solving for two of the

https://doi.org/10.1017/S0263574718000826 Published online by Cambridge University Press

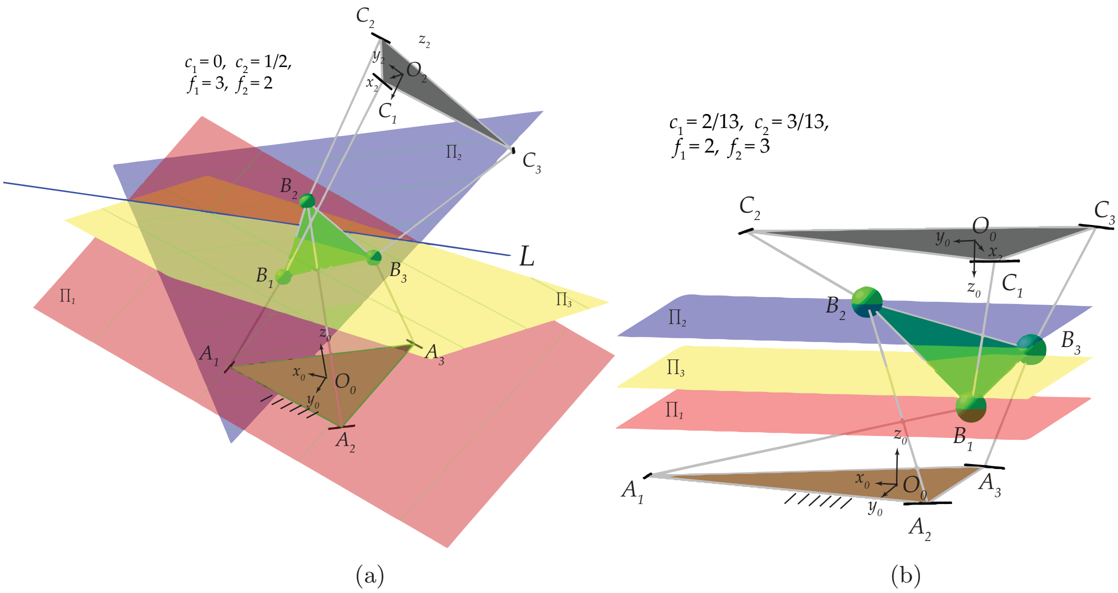

Fig. 6. Serial singular configurations when three sides of the characteristic tetrahedron meet in a line. (a) A real line L. (b) A line at infinity.

four parameters c_1, c_2, f_1 and f_2:

$$\left.\begin{array}{l}\mathbf{T}(2,4) = -\mathbf{T}(4,2) = 0 \\ \mathbf{T}(3,4) = -\mathbf{T}(4,3) = 0\end{array}\right\} \Longrightarrow \begin{array}{c} f_1 = \dfrac{c_1}{c_1^2 + c_2^2},\ f_2 = \dfrac{c_2}{c_1^2 + c_2^2} \\ \text{OR} \\ c_1 = \dfrac{f_1}{f_1^2 + f_2^2},\ c_2 = \dfrac{f_2}{f_1^2 + f_2^2} \end{array} \tag{38}$$

The relations in Eq. (38) satisfy the equation $c_1 f_1 + c_2 f_2 - 1 = 0$. Hence, this equation is a necessary and a sufficient condition for three sides to have a common line of intersection and it instantaneously reduces the dof of the S–PM at hand by 1. Furthermore, by substituting Eq. (38) in $\mathbf{T}$, the magnitude of rotation about the z_0-axis is given by $\sigma = \tan^{-1}(\dfrac{2c_1c_2}{c_2^2 - c_1^2}) = \tan^{-1}(\dfrac{2f_1f_2}{f_2^2 - f_1^2})$. A serial singular configuration in which $\sigma = 67°$ is shown in Fig. 6b. Note that in theory the platform can have an upright position or an upside down position and yet stay parallel to the base.

Case 3: Two sides and base meet in a line: Considering a side plane Π_i, $i = 1, 2, 3$ and the base plane Π_4, their line of intersection must pass through B_i. To prove if Π_i, Π_j and Π_4, $i, j = 1, 2, 3$ have a common line of intersection, it is sufficient to prove that the points B_i and B_j simultaneously lie on the planes Π_j and Π_i, respectively. If there exists a line common to all the three planes, it should be along B_iB_j as shown in Fig. 7. For instance, if planes Π_1, Π_2 and Π_4 are considered, simultaneous incidence of point B_1 on Π_2 and that of point B_2 on Π_1 must be satisfied and is expressed by the following equations:

$$\mathbf{r}_{B_1} \cdot ([w_{02},\ \mathbf{w}_2]) = 0 \Longrightarrow$$

$$-2\sqrt{3}c_1c_2f_1 - 2\sqrt{3}c_1f_1f_2 + 3\,{c_1}^2f_1 + 3\,{f_1}^2c_1 - 3\,{f_2}^2c_1 - 3\,{c_2}^2f_1 - 3\,c_1 - 3\,f_1 = 0 \tag{39}$$

$$\mathbf{r}_{B_2} \cdot ([w_{01},\ \mathbf{w}_1]) = 0 \Longrightarrow$$

$$-4\sqrt{3}c_1c_2f_2 - 4\sqrt{3}c_2f_1f_2 + 4\,c_2c_1f_1 + 4\,f_2c_1f_1 + c_1\sqrt{3} + \sqrt{3}f_1 - 3\,c_2 - 3\,f_2 = 0 \tag{40}$$

https://doi.org/10.1017/S0263574718000826 Published online by Cambridge University Press

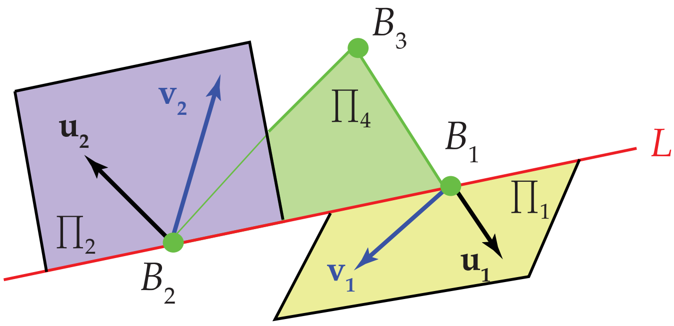

Fig. 7. Can two sides and base of the characteristic tetrahedron of the 3-RPS-3-SPR S–PM meet in a line?

Finding the Groebner basis of the polynomials in Eqs. (39) and (40) with a graded reverse lexicographic ordering (*tdeg* in Maple) of the parameters $c_1 <_{\text{grlex}} c_2 <_{\text{grlex}} f_1 <_{\text{grlex}} f_2$, results in a basis of four polynomials. The four equations can then be solved for c_1, c_2, f_1 and f_2. Two solutions are obtained, the first one turns out to be a complex solution and the second one is exactly the last case of (29). The second solution should also be rejected since it is assumed for this analysis that none of the faces of the characteristic tetrahedron degenerates into a line. Also for other combinations of sides and their intersections with the base plane, the following equations are solved for the parameters:

$$\mathbf{r}_{B_2} \cdot ([w_{03},\ \mathbf{w}_3]) = 0 \implies$$
$$3\,{c_1}^2 f_2 - 2\,c_1 c_2 f_1 - 2\,c_1 f_1 f_2 - 3\,{c_2}^2 f_2 + 3\,c_2 {f_1}^2 - 3\,c_2 {f_2}^2 + 3\,c_2 + 3\,f_2 = 0 \tag{41}$$
$$\mathbf{r}_{B_3} \cdot ([w_{02},\ \mathbf{w}_2]) = 0 \implies$$
$${c_1}^2 f_1 - 2\,c_1 c_2 f_2 + c_1 {f_1}^2 - c_1 {f_2}^2 - {c_2}^2 f_1 - 2\,c_2 f_1 f_2 + c_1 + f_1 = 0 \tag{42}$$
$$\mathbf{r}_{B_1} \cdot ([w_{03},\ \mathbf{w}_3]) = 0 \implies$$
$$-4\sqrt{3}c_1 c_2 f_2 - 4\sqrt{3}c_2 f_1 f_2 - 4\,c_1 c_2 f_1 - 4\,c_1 f_1 f_2 + c_1\sqrt{3} + \sqrt{3} f_1 + 3\,c_2 + 3\,f_2 = 0 \tag{43}$$
$$\mathbf{r}_{B_3} \cdot ([w_{01},\ \mathbf{w}_1]) = 0 \implies$$
$$2\sqrt{3}c_1 c_2 f_1 + 2\sqrt{3}c_1 f_1 f_2 + 3\,{c_1}^2 f_1 + 3\,c_1 {f_1}^2 - 3\,c_1 {f_2}^2 - 3\,{c_2}^2 f_1 - 3\,c_1 - 3\,f_1 = 0 \tag{44}$$

In each case, the solutions obtained are either complex or correspond to the last case of (29), showing that the S–PM at hand cannot have a configuration in which any two sides and the base of its characteristic tetrahedron meet in a line.

Another approach to solve this case is by finding the condition for incidence of an intersection line between two sides and the base:[33]

$$L_{ij} : (\mathbf{l}_{ij},\ \bar{\mathbf{l}}_{ij}) = (\mathbf{w}_i \times \mathbf{w}_j,\ \ w_{0i}\mathbf{w}_j - w_{0j}\mathbf{w}_i) \tag{45}$$
$$\Pi_4 \wedge L_{ij} = 0 : \mathbf{w}_4 \cdot \mathbf{l}_{ij} = 0, \quad -w_{03}\mathbf{l}_{ij} + \mathbf{w}_4 \times \bar{\mathbf{l}}_{ij} = 0, \quad i = 1, 2, 3 \tag{46}$$

Equation (46) does not yield any real or non-trivial solutions. As a result, it is proved by contradiction that the 3-RPS-3-SPR S–PM cannot have a serial singular configuration in which any two sides and the base of the characteristic tetrahedron meet in a line.

Cases 4 and above: The remaining cases in Table 1 of ref. [22] include two sides meet in a plane, one side and base meet in a plane, two sides and base meet in a plane, two faces meet in a plane. Since the S–PM cannot attain a configuration of Case 3, it is certain that it cannot reach any configuration corresponding to the remaining cases. For example, if two sides could meet in a plane, this case should have appeared as a solution to Eqs. (39) and (40) and in which case, there definitely would have existed a line of intersection between the meeting plane and the base.

To this end, all possible serial singularities are listed in Table I.

https://doi.org/10.1017/S0263574718000826 Published online by Cambridge University Press

https://doi.org/10.1017/S0263574718000826 Published online by Cambridge University Press

Table I. Enumeration of serial singularities for the 3-RPS-3-SPR S–PM.

Geometrical condition	Algebraic expression	Instantaneous *dof*	An example configuration
Parallel revolute joints			
i. ${}^0\mathbf{u_1} \,\|\|\, {}^0\mathbf{v_1}$	$c_1 = 0,\ f_1 = 0$	5	Figure 3a
ii. ${}^0\mathbf{u_2} \,\|\|\, {}^0\mathbf{v_2}$	$c_1 = -\sqrt{3}c_2,\ f_1 = -\sqrt{3}f_2$	5	Figure 3b
iii. ${}^0\mathbf{u_3} \,\|\|\, {}^0\mathbf{v_3}$	$c_1 = \sqrt{3}c_2,\ f_1 = \sqrt{3}f_2$	5	Figure 3c
iv. Parallel base and platform (platform pure translation) ${}^0\mathbf{u_i} \,\|\|\, {}^0\mathbf{v_i} \quad \forall i = 1, 2, 3$	$c_1 = -f_1,\ c_2 = -f_2$	3	Figure 3d
Degeneracy of the characteristic tetrahedron[22]			
vi. Four faces meet in a point (general linear complex[32])			
a. A real point	$p^7(c_1, c_2, f_1, f_2) = 0$ (Eq. (31))	5	Figure 5a
b. A point at infinity	$c_1 = -\dfrac{f_1}{f_1^2 + f_2^2},\ c_2 = -\dfrac{f_2}{f_1^2 + f_2^2}$	5	Figure 5b
vi. Three sides meet in a line (special linear complex)			
a. A real line	$c_1 f_1 + c_2 f_2 - 1 = 0$	5	Figure 6a
b. A line at infinity parallel base and platform (rotation about z_0-axis)	$c_1 = \dfrac{f_1}{f_1^2 + f_2^2},\ c_2 = \dfrac{f_2}{f_1^2 + f_2^2}$	5	Figure 6b

It is recalled here that the singularity analysis performed in this section is by considering both modules in the OM corresponding to $c_3 = f_3 = 0$. In fact, there are three other possibilities, $c_0 = f_0 = 0, c_0 = f_3 = 0$ and $c_3 = f_0 = 0$. For these cases, the algebraic expressions for serial singularities can be obtained by the following replacements to the ones listed in Table I. These replacements hold true only for the orientation parameters. Favourably, the serial singular configurations for $f_3 = c_3 = 0$ expressed in Table I are only functions of orientation parameters $c_i, f_i, i = 1, 2$.

$$
\begin{aligned}
&Case\ \ a.\ \ c_3 = f_3 = 0 : \text{Listed in Table I}\\
&Case\ \ b.\ \ c_0 = f_0 = 0 : f_2 \to -f_1, f_1 \to f_2,\ c_1 \to -c_2, c_2 \to c_1\\
&Case\ \ c.\ \ c_0 = f_3 = 0 : c_1 \to -c_2, c_2 \to c_1\\
&Case\ \ d.\ \ c_0 = f_3 = 0 : f_2 \to -f_1, f_1 \to f_2
\end{aligned}
\tag{47}
$$

Proof: For the three-RPS ($f_i, i = 0, 1, 2, 3$) and the three-SPR ($c_i, i = 0, 1, 2, 3$) parallel manipulator modules, the orientation study parameters can be expressed in terms of the *Tilt and Torsion* angles,[34] azimuth (ϕ), tilt (θ) and torsion (σ) as follows:

$$
\begin{aligned}
f_0 &= \cos(\frac{\theta_1}{2})\cos(\frac{\sigma_1}{2}) & c_0 &= \cos(\frac{\theta_2}{2})\cos(\frac{\sigma_2}{2})\\
f_1 &= \sin(\frac{\theta_1}{2})\cos(\phi_1 - \frac{\sigma_1}{2}) & c_1 &= -\sin(\frac{\theta_2}{2})\cos(\phi_2 - \frac{\sigma_2}{2})\\
f_2 &= \sin(\frac{\theta_1}{2})\sin(\phi_1 - \frac{\sigma_1}{2}) & c_2 &= -\sin(\frac{\theta_2}{2})\sin(\phi_2 - \frac{\sigma_2}{2})\\
f_3 &= \cos(\frac{\theta_1}{2})\sin(\frac{\sigma_1}{2}) & c_3 &= -\cos(\frac{\theta_2}{2})\sin(\frac{\sigma_2}{2})
\end{aligned}
\tag{48}
$$

The OM $c_0 = 0$ or $f_0 = 0$ renders the torsion angle $\sigma_1 = 0$ or $\sigma_2 = 0$ and if $f_3 = 0$ or $c_3 = 0, \sigma_1 = 180^\circ$ or $\sigma_2 = 180^\circ$, respectively. Furthermore, if, for instance in the OM corresponding to $f_0 = 0$, the three-RPS PM can never have $f_3 = 0$, thus the parameters $f_i, i = 0, 1, 2, 3$ can be normalized by forcing $f_3 = 1$. Consequently, the OM as functions of tilt and azimuth angles can be represented for each module as follows:

$$
\begin{aligned}
&\text{Three-RPS OM-1} && \text{Three-SPR OM-1}\\
&f_0 = 1 && c_0 = 1\\
&f_1 = \tan(\frac{\theta_1}{2})\cos(\phi_1) && c_1 = -\tan(\frac{\theta_2}{2})\cos(\phi_2)\\
&f_2 = \tan(\frac{\theta_1}{2})\sin(\phi_1) && c_2 = -\tan(\frac{\theta_2}{2})\sin(\phi_2)\\
&f_3 = 0 && c_3 = 0\\
&\text{Three-RPS OM-2} && \text{Three-SPR OM-2}\\
&f_0 = 0 && c_0 = 0\\
&f_1 = \tan(\frac{\theta_1}{2})\sin(\phi_1) && c_1 = -\tan(\frac{\theta_2}{2})\sin(\phi_2)\\
&f_2 = -\tan(\frac{\theta_1}{2})\cos(\phi_1) && c_2 = \tan(\frac{\theta_2}{2})\cos(\phi_2)\\
&f_3 = 1 && c_3 = 1
\end{aligned}
\tag{49}
$$

https://doi.org/10.1017/S0263574718000826 Published online by Cambridge University Press

Thus, it is obvious that for the three-RPS PM, algebraic expressions in OM-2 can be obtained from those in OM-1 by replacing $f_2 \to -f_1$ and $f_1 \to f_2$. For the three-SPR PM, these replacements will be $c_2 \to c_1$ and $c_1 \to -c_2$. Accordingly, all the serial singular configurations of the 3-RPS-3-SPR PM can be enumerated starting from *Case a* (where both modules are in OM-1) of Eq. (47).

5. Direct Kinematics Model (DKM)

The six prismatic joints of the 3-RPS-3-SPR S–PM are assumed to be actuated. Direct kinematics gives the pose, i.e., the position and orientation, of the moving platform for given prismatic joint lengths. For the three-RPS and the three-SPR PMs, the prismatic joint lengths are named as p_1, p_2, p_3 and q_1, q_2, q_3, respectively. If study parameters $x_0, x_1, x_2, x_3, y_0, y_1, y_2$ and y_3 represent the pose of the moving platform relative to the base, the direct kinematics problem aims to find x_i and y_i, $i = 0, 1, 2, 3$ given p_j and q_j, $j = 1, 2, 3$.

As mentioned in Section 3, the transformation matrix between the fixed base and the moving platform, $\mathbf{T}$ is determined to be a function of f_1, f_2, g_1, c_1, c_2 and d_1 for the case $c_3 = f_3 = 0$. Therefore, the sphere constraint equations[21] for each module after factoring out the non-zero terms are expressed as follows:

$$
\begin{aligned}
&||\,{}^0\mathbf{r}_{B_i} - {}^0\mathbf{r}_{A_i}||^2 = p_i^2 \quad i = 1, 2, 3 \implies \\
&S_1 := \left(-p_1{}^2 + h_0{}^2 - 4\,h_0 h_1 + 4\,h_1{}^2\right) f_1{}^4 f_2{}^2 + 4\,f_1{}^4 g_1{}^2 + 4\,h_1 f_1{}^4 g_1 + h_1{}^2 f_1{}^4 \\
&\quad + (-2\,p_1{}^2 + 2\,h_0{}^2 - 8\,h_1{}^2) f_1{}^2 f_2{}^4 + 8\,f_1{}^2 f_2{}^2 g_1{}^2 - 8\,h_1 f_1{}^2 f_2{}^2 g_1 + (-2\,p_1{}^2 \\
&\quad + 2\,h_0{}^2 - 6\,h_0 h_1 - 2\,h_1{}^2) f_1{}^2 f_2{}^2 + 8\,f_1{}^2 g_1{}^2 + 4\,h_1 f_1{}^2 g_1 + (-p_1{}^2 + h_0{}^2 \\
&\quad + 4\,h_0 h_1 + 4\,h_1{}^2) f_2{}^6 + 4\,f_2{}^4 g_1{}^2 - 12\,h_1 f_2{}^4 g_1 + (-2\,p_1{}^2 + 2\,h_0{}^2 + 2\,h_0 h_1 \\
&\quad + 5\,h_1{}^2) f_2{}^4 + 8\,f_2{}^2 g_1{}^2 - 12\,h_1 f_2{}^2 g_1 + \left(-p_1{}^2 + h_0{}^2 - 2\,h_0 h_1 + h_1{}^2\right) f_2{}^2 \\
&\quad + 4\,g_1{}^2 = 0
\end{aligned} \tag{50}
$$

$$
\begin{aligned}
S_2 &:= \left(4\,h_0{}^2 + 8\,h_0 h_1 + 4\,h_1{}^2 - 4\,p_2{}^2\right) f_1{}^4 f_2{}^2 + 16\,f_1{}^4 g_1{}^2 + 16\,h_1 f_1{}^4 g_1 + 4\,h_1{}^2 f_1{}^4 \\
&\quad + \left(16\sqrt{3}h_0 h_1 + 16\sqrt{3}h_1{}^2\right) f_1{}^3 f_2{}^3 + 16\sqrt{3} f_1{}^3 f_2 g_1 h_1 + 8\sqrt{3} f_1{}^3 f_2 h_1{}^2 \\
&\quad + \left(8\,h_0{}^2 + 40\,h_1{}^2 - 8\,p_2{}^2\right) f_1{}^2 f_2{}^4 + 32\,f_1{}^2 f_2{}^2 g_1{}^2 + 16\,h_1 f_1{}^2 f_2{}^2 g_1 + (8\,h_0{}^2 \\
&\quad + 4\,h_1{}^2 - 8\,p_2{}^2) f_1{}^2 f_2{}^2 + 32\,f_1{}^2 g_1{}^2 + 16\,h_1 f_1{}^2 g_1 + (16\sqrt{3}h_0 h_1 \\
&\quad - 16\sqrt{3}h_1{}^2) f_1 f_2{}^5 + 16\sqrt{3} f_1 f_2{}^3 g_1 h_1 + \left(16\sqrt{3}h_0 h_1 - 16\sqrt{3}h_1{}^2\right) f_1 f_2{}^3 \\
&\quad + 16\sqrt{3} f_1 f_2 g_1 h_1 + \left(4\,h_0{}^2 - 8\,h_0 h_1 + 4\,h_1{}^2 - 4\,p_2{}^2\right) f_2{}^6 + 16\,f_2{}^4 g_1{}^2 \\
&\quad + \left(8\,h_0{}^2 - 16\,h_0 h_1 + 8\,h_1{}^2 - 8\,p_2{}^2\right) f_2{}^4 + 32\,f_2{}^2 g_1{}^2 + (4\,h_0{}^2 - 8\,h_0 h_1 \\
&\quad + 4\,h_1{}^2 - 4\,p_2{}^2) f_2{}^2 + 16\,g_1{}^2 = 0
\end{aligned} \tag{51}
$$

$$
\begin{aligned}
S_3 &:= \left(4\,h_0{}^2 + 8\,h_0 h_1 + 4\,h_1{}^2 - 4\,p_3{}^2\right) f_1{}^4 f_2{}^2 + 16\,f_1{}^4 g_1{}^2 + 16\,h_1 f_1{}^4 g_1 + 4\,h_1{}^2 f_1{}^4 \\
&\quad + \left(-16\sqrt{3}h_0 h_1 - 16\sqrt{3}h_1{}^2\right) f_1{}^3 f_2{}^3 - 16\sqrt{3} f_1{}^3 f_2 g_1 h_1 - 8\sqrt{3} f_1{}^3 f_2 h_1{}^2 \\
&\quad + \left(8\,h_0{}^2 + 40\,h_1{}^2 - 8\,p_3{}^2\right) f_1{}^2 f_2{}^4 + 32\,f_1{}^2 f_2{}^2 g_1{}^2 + 16\,h_1 f_1{}^2 f_2{}^2 g_1 + (8\,h_0{}^2 \\
&\quad + 4\,h_1{}^2 - 8\,p_3{}^2) f_1{}^2 f_2{}^2 + 32\,f_1{}^2 g_1{}^2 + 16\,h_1 f_1{}^2 g_1 + (-16\sqrt{3}h_0 h_1 \\
&\quad + 16\sqrt{3}h_1{}^2) f_1 f_2{}^5 - 16\sqrt{3} f_1 f_2{}^3 g_1 h_1 + \left(-16\sqrt{3}h_0 h_1 + 16\sqrt{3}h_1{}^2\right) f_1 f_2{}^3 \\
&\quad - 16\sqrt{3} f_1 f_2 g_1 h_1 + \left(4\,h_0{}^2 - 8\,h_0 h_1 + 4\,h_1{}^2 - 4\,p_3{}^2\right) f_2{}^6 + 16\,f_2{}^4 g_1{}^2 \\
&\quad + \left(8\,h_0{}^2 - 16\,h_0 h_1 + 8\,h_1{}^2 - 8\,p_3{}^2\right) f_2{}^4 + 32\,f_2{}^2 g_1{}^2 + (4\,h_0{}^2 - 8\,h_0 h_1 \\
&\quad + 4\,h_1{}^2 - 4\,p_3{}^2) f_2{}^2 + 16\,g_1{}^2 = 0
\end{aligned} \tag{52}
$$

https://doi.org/10.1017/S0263574718000826 Published online by Cambridge University Press

$$||{}^0\mathbf{r}_{C_i} - {}^0\mathbf{r}_{B_i}||^2 = q_i^2 \quad i = 1, 2, 3 \implies$$

$$\begin{aligned} S_4 :=& \left(4\,h_1^{\,2} - 4\,h_1h_2 + h_2^{\,2} - q_1^{\,2}\right) c_1^{\,4}c_2^{\,2} + 4\,c_1^{\,4}d_1^{\,2} - 4\,c_1^{\,4}d_1h_1 + c_1^{\,4}h_1^{\,2} \\ &+ \left(-8\,h_1^{\,2} + 2\,h_2^{\,2} - 2\,q_1^{\,2}\right) c_1^{\,2}c_2^{\,4} + 8\,c_1^{\,2}c_2^{\,2}d_1^{\,2} + 8\,c_1^{\,2}c_2^{\,2}d_1h_1 + (-2\,h_1^{\,2} \\ &- 6\,h_1h_2 + 2\,h_2^{\,2} - 2\,q_1^{\,2})c_1^{\,2}c_2^{\,2} + 8\,c_1^{\,2}d_1^{\,2} - 4\,c_1^{\,2}d_1h_1 + (4\,h_1^{\,2} + 4\,h_1h_2 \\ &+ h_2^{\,2} - q_1^{\,2})c_2^{\,6} + 4\,c_2^{\,4}d_1^{\,2} + 12\,c_2^{\,4}d_1h_1 + (5\,h_1^{\,2} + 2\,h_1h_2 + 2\,h_2^{\,2} \\ &- 2\,q_1^{\,2})c_2^{\,4} + 8\,c_2^{\,2}d_1^{\,2} + 12\,c_2^{\,2}d_1h_1 + \left(h_1^{\,2} - 2\,h_1h_2 + h_2^{\,2} - q_1^{\,2}\right) c_2^{\,2} \\ &+ 4\,d_1^{\,2} = 0 \end{aligned} \tag{53}$$

$$\begin{aligned} S_5 :=& \left(h_1^{\,2} + 2\,h_1h_2 + h_2^{\,2} - q_2^{\,2}\right) c_1^{\,4}c_2^{\,2} + 4\,c_1^{\,4}d_1^{\,2} - 4\,c_1^{\,4}d_1h_1 + c_1^{\,4}h_1^{\,2} \\ &+ \left(4\sqrt{3}h_1^{\,2} + 4\sqrt{3}h_1h_2\right) c_1^{\,3}c_2^{\,3} - 4\sqrt{3}c_1^{\,3}c_2d_1h_1 + 2\sqrt{3}c_1^{\,3}c_2h_1^{\,2} \\ &+ \left(10\,h_1^{\,2} + 2\,h_2^{\,2} - 2\,q_2^{\,2}\right) c_1^{\,2}c_2^{\,4} + 8\,c_1^{\,2}c_2^{\,2}d_1^{\,2} - 4\,c_1^{\,2}c_2^{\,2}d_1h_1 + (h_1^{\,2} \\ &+ 2\,h_2^{\,2} - 2\,q_2^{\,2})c_1^{\,2}c_2^{\,2} + 8\,c_1^{\,2}d_1^{\,2} - 4\,c_1^{\,2}d_1h_1 + (-4\sqrt{3}h_1^{\,2} \\ &+ 4\sqrt{3}h_1h_2)c_1c_2^{\,5} - 4\sqrt{3}c_1c_2^{\,3}d_1h_1 + \left(-4\sqrt{3}h_1^{\,2} + 4\sqrt{3}h_1h_2\right) c_1c_2^{\,3} \\ &- 4\sqrt{3}c_1c_2d_1h_1 + \left(h_1^{\,2} - 2\,h_1h_2 + h_2^{\,2} - q_2^{\,2}\right) c_2^{\,6} + 4\,c_2^{\,4}d_1^{\,2} + (2\,h_1^{\,2} \\ &- 4\,h_1h_2 + 2\,h_2^{\,2} - 2\,q_2^{\,2})c_2^{\,4} + 8\,c_2^{\,2}d_1^{\,2} + \left(h_1^{\,2} - 2\,h_1h_2 + h_2^{\,2} - q_2^{\,2}\right) c_2^{\,2} \\ &+ 4\,d_1^{\,2} = 0 \end{aligned} \tag{54}$$

$$\begin{aligned} S_6 :=& \left(-h_1^{\,2} - 2\,h_1h_2 - h_2^{\,2} + q_3^{\,2}\right) c_1^{\,4}c_2^{\,2} - 4\,c_1^{\,4}d_1^{\,2} + 4\,c_1^{\,4}d_1h_1 - c_1^{\,4}h_1^{\,2} \\ &+ \left(4\sqrt{3}h_1^{\,2} + 4\sqrt{3}h_1h_2\right) c_1^{\,3}c_2^{\,3} - 4\sqrt{3}c_1^{\,3}c_2d_1h_1 + 2\sqrt{3}c_1^{\,3}c_2h_1^{\,2} \\ &+ \left(-10\,h_1^{\,2} - 2\,h_2^{\,2} + 2\,q_3^{\,2}\right) c_1^{\,2}c_2^{\,4} - 8\,c_1^{\,2}c_2^{\,2}d_1^{\,2} + 4\,c_1^{\,2}c_2^{\,2}d_1h_1 + (-h_1^{\,2} \\ &- 2\,h_2^{\,2} + 2\,q_3^{\,2})c_1^{\,2}c_2^{\,2} - 8\,c_1^{\,2}d_1^{\,2} + 4\,c_1^{\,2}d_1h_1 + (-4\sqrt{3}h_1^{\,2} \\ &+ 4\sqrt{3}h_1h_2)c_1c_2^{\,5} - 4\sqrt{3}c_1c_2^{\,3}d_1h_1 + \left(-4\sqrt{3}h_1^{\,2} + 4\sqrt{3}h_1h_2\right) c_1c_2^{\,3} \\ &- 4\sqrt{3}c_1c_2d_1h_1 + \left(-h_1^{\,2} + 2\,h_1h_2 - h_2^{\,2} + q_3^{\,2}\right) c_2^{\,6} - 4\,c_2^{\,4}d_1^{\,2} + (-2\,h_1^{\,2} \\ &+ 4\,h_1h_2 - 2\,h_2^{\,2} + 2\,q_3^{\,2})c_2^{\,4} - 8\,c_2^{\,2}d_1^{\,2} + \left(-h_1^{\,2} + 2\,h_1h_2 - h_2^{\,2} + q_3^{\,2}\right) c_2^{\,2} \\ &- 4\,d_1^{\,2} = 0 \end{aligned} \tag{55}$$

By substituting the prismatic joint lengths p_i and q_i, Eqs. (50) to (55) can be solved for the parameters f_1, f_2, g_1, c_1, c_2 and d_1. Since each module can have up to eight direct kinematics solutions[21,24] in each OM, the 3-RPS-3-SPR S–PM can have up to 64 solutions for its direct kinematics problem in each case of Eq. (47). The transformation matrix between the fixed frame $\mathcal{F}_0$ and the moving platform frame $\mathcal{F}_2$ is established as $\mathbf{T}$ in Section 3. By expressing this matrix in dual quaternion form or mapping it to a point in $\mathbb{P}^7$ leads to the representation of the S–PM at hand in terms of the orientation study parameters x_i, $i = 0, 1, 2, 3$ as follows:

$$\begin{bmatrix} x_0 \\ x_1 \\ x_2 \\ x_3 \end{bmatrix} = \begin{bmatrix} c_1f_1 + c_2f_2 - 1 \\ -c_1 - f_1 \\ -c_2 - f_2 \\ c_1f_2 - c_2f_1 \end{bmatrix} \tag{56}$$

The expressions for the translational study parameters y_i, $i = 0, 1, 2, 3$ as a function of f_1, f_2, g_1, c_1, c_2 and d_1 are shown in the Appendix. Note that every term in the right-hand side of Eq. (56) is divided

https://doi.org/10.1017/S0263574718000826 Published online by Cambridge University Press

by $c_1 f_1 + c_2 f_2 - 1 \neq 0$. The case $c_1 f_1 + c_2 f_2 - 1 = 0$ is a particular singularity condition identified as the case vi. a. in Table I. It is easy to verify from Eqs. (56) and (A1) that the study parameters x_i, y_i, $i = 0, 1, 2, 3$ satisfy the study's quadric equation:

$$x_0 y_0 + x_1 y_1 + x_2 y_2 + x_3 y_3 = 0 \tag{57}$$

The Plücker coordinates $(p_{01}, p_{02}, p_{03}, p_{23}, p_{31}, p_{12})$ of the corresponding *Finite Screw Axis* (FSA) are given by[35]

$$\begin{aligned} p_{01} &= (-x_1^2 - x_2^2 - x_3^2)x_1, & p_{23} &= x_0 y_0 x_1 - (-x_1^2 - x_2^2 - x_3^2)y_1 \\ p_{02} &= (-x_1^2 - x_2^2 - x_3^2)x_2, & p_{31} &= x_0 y_0 x_2 - (-x_1^2 - x_2^2 - x_3^2)y_2 \\ p_{03} &= (-x_1^2 - x_2^2 - x_3^2)x_3, & p_{12} &= x_0 y_0 x_3 - (-x_1^2 - x_2^2 - x_3^2)y_3 \end{aligned} \tag{58}$$

The following conclusions are drawn from Eqs. (56) and (58):

- $x_0 = 0$ implies that the transformation is a finite screw motion[21] with an angle of 180°, also called as a π screw by Study. It corresponds to the singularity condition vi. in Table I.
- $x_1 = x_2 = 0$ makes $p_{01} = p_{02} = 0$, implying that the direction of the FSA is vertical. It corresponds to the singularity condition iv. in Table I where the platform and the base are parallel to each other.
- $x_3 = 0$ makes $p_{03} = 0$, implying that the FSA is parallel to the $x_0 y_0$ plane. In this case, $c_1 f_2 = c_2 f_1$. If $c_1 = 0$, then it corresponds to the singular configuration i. in Table I.

In fact, the direct kinematics problem is solved by first calculating the parameters $f_1, f_2, g_1, c_1, c_2, d_1$ and then finding the study parameters x_i, y_i, $i = 0, 1, 2, 3$ of the whole S–PM. To derive six equations in input prismatic joint lengths p_j, q_j, $j = 1, 2, 3$ and output study parameters x_i, y_i, $i = 0, 1, 2, 3$ is algebraically cumbersome and is still an open problem.

6. Inverse Kinematics Model (IKM)

The inverse kinematics problem of the manipulator under study aims at finding the prismatic joint lengths as a function of the moving platform pose. Given the study parameters, x_i, y_i, $i = 0, 1, 2, 3$ representing the transformation between the moving platform and the fixed base, the prismatic joint lengths p_j, q_j, $j = 1, 2, 3$ must be determined. In other words, given points C_i and A_i, point B_i, $i = 1, 2, 3$ (refer Fig. 1) must be determined.

Let the given transformation matrix between the fixed frame $\mathcal{F}_0$ and the moving platform frame $\mathcal{F}_2$ be $\mathbf{M}$. Thus, the coordinates of point C_i expressed in $\mathcal{F}_2$ as shown in Eq. (18) can be represented in $\mathcal{F}_0$ as ${}^0\mathbf{r}_{C_i} = \mathbf{M}\,{}^2\mathbf{r}_{C_i}$. Let the homogeneous coordinates of point B_i expressed in coordinate frame $\mathcal{F}_0$ be ${}^0\mathbf{r}_{B_i} = [1, Bx_i, By_i, Bz_i]$. The homogeneous coordinates of planes α_i and β_i shown in Fig. 1 are

$$\begin{aligned} \alpha_i &: [-\mathbf{r}_{A_i}^T \mathbf{u}_i,\ \ \mathbf{u}_i^T] \\ \beta_i &: [-\mathbf{r}_{C_i}^T \mathbf{v}_i,\ \ \mathbf{v}_i^T] \end{aligned}$$

where all the vectors are expressed in frame $\mathcal{F}_0$. To determine the points B_i, the constraints to be respected are point B_i must lie in the plane α_i and β_i simultaneously and the distance between points B_i and B_j, $i \neq j = 1, 2, 3$ must be equal to the side length of the coupler triangular platform, $\sqrt{3}h_1$, h_1 being the circum-radius. Three constraints in each leg lead to a total of nine algebraic constraint

https://doi.org/10.1017/S0263574718000826 Published online by Cambridge University Press

Table II. Solutions to inverse kinematics of the 3-RPS-3-SPR S–PM when $h_0 = 2, h_1 = 1, h_2 = 2$ and $(x_0 : x_1 : x_2 : x_3 : y_0 : y_1 : y_2 : y_3) = (2.8215 : -1.2912 : -0.3348 : 1.2434 : 2.1837 : 1.1542 : 1.6012 : -3.3256)$.

IKM solution	Bx_1	By_1	Bz_1	Bx_2	By_2	Bz_2	Bx_3	By_3	Bz_3
1	1.190	0.0	1.095	0.922	−1.597	1.710	− 0.398	− 0.689	1.051
2	−0.385	0.0	2.289	−0.049	0.084	3.986	−0.773	−1.339	3.317
3	−0.867	0.0	2.650	0.562	−0.972	2.550	−0.412	−0.712	1.140
4	−1.500	0.0	3.130	0.169	−0.293	3.470	−0.564	−0.976	2.060
5	0.893	0.0	1.320	0.991	−1.710	1.540	− 0.517	−0.895	1.780
6	−1.080	0.0	2.810	0.461	−0.797	2.790	− 0.841	−1.450	3.720
7	1.210	0.0	1.080	0.724	−1.250	2.170	−0.384	−0.665	0.975
8	−1.600	0.0	3.210	−0.032	0.055	3.940	−0.845	−1.460	3.750

equations:

Point B_i belongs to plane α_i:

$$F_1 := By_1 = 0 \tag{59}$$

$$F_2 := -\sqrt{3}Bx_2 - By_2 \tag{60}$$

$$F_3 := \sqrt{3}Bx_3 - By_3 \tag{61}$$

Point B_i belongs to plane β_i:

$$F_4 := (-2\,x_0x_3 + 2\,x_1x_2)\,Bx_1 + \left(x_0{}^2 - x_1{}^2 + x_2{}^2 - x_3{}^2\right)By_1 + (2\,x_0x_1 + 2\,x_2x_3)Bz_1 + 2\,x_0y_2 + 2\,x_1y_3 - 2\,x_2y_0 - 2\,x_3y_1 = 0 \tag{62}$$

$$F_5 := \left(-\sqrt{3}x_0{}^2 - \sqrt{3}x_1{}^2 + \sqrt{3}x_2{}^2 + \sqrt{3}x_3{}^2 + 2\,x_0x_3 - 2\,x_1x_2\right)Bx_2 + (-2\,\sqrt{3}x_0x_3 - 2\,\sqrt{3}x_1x_2 - x_0{}^2 + x_1{}^2 - x_2{}^2 + x_3{}^2)By_2 + (2\,\sqrt{3}x_0x_2 - 2\,\sqrt{3}x_1x_3 - 2\,x_0x_1 - 2\,x_2x_3)Bz_2 - 2\,\sqrt{3}x_0y_1 + 2\,\sqrt{3}x_1y_0 + 2\,\sqrt{3}x_2y_3 - 2\,\sqrt{3}x_3y_2 - 2\,x_0y_2 - 2\,x_1y_3 + 2\,x_2y_0 + 2\,x_3y_1 = 0 \tag{63}$$

$$F_6 := \left(\sqrt{3}x_0{}^2 + \sqrt{3}x_1{}^2 - \sqrt{3}x_2{}^2 - \sqrt{3}x_3{}^2 + 2\,x_0x_3 - 2\,x_1x_2\right)Bx_3 + (2\,\sqrt{3}x_0x_3 + 2\,\sqrt{3}x_1x_2 - x_0{}^2 + x_1{}^2 - x_2{}^2 + x_3{}^2)By_3 + (-2\,\sqrt{3}x_0x_2 + 2\,\sqrt{3}x_1x_3 - 2\,x_0x_1 - 2\,x_2x_3)Bz_3 + 2\,\sqrt{3}x_0y_1 - 2\,\sqrt{3}x_1y_0 - 2\,\sqrt{3}x_2y_3 + 2\,\sqrt{3}x_3y_2 - 2\,x_0y_2 - 2\,x_1y_3 + 2\,x_2y_0 + 2\,x_3y_1 \tag{64}$$

$$||\mathbf{r}_{B_i} - \mathbf{r}_{B_j}||^2 = 3h_1^2 \quad i \neq j = 1, 2, 3 \implies$$

$$F_7 := (Bx_1 - Bx_2)^2 + \left(By_1 - By_2\right)^2 + (Bz_1 - Bz_2)^2 - 3\,h_1{}^2 = 0 \tag{65}$$

$$F_8 := (Bx_1 - Bx_3)^2 + \left(By_1 - By_3\right)^2 + (Bz_1 - Bz_3)^2 - 3\,h_1{}^2 = 0 \tag{66}$$

$$F_9 := (Bx_2 - Bx_3)^2 + \left(By_2 - By_3\right)^2 + (Bz_2 - Bz_3)^2 - 3\,h_1{}^2 = 0 \tag{67}$$

$F_i, i = 1, \ldots, 9$ can be solved for the nine parameters Bx_j, By_j and Bz_j, $j = 1, 2, 3$ to further obtain the prismatic joint lengths.

After substituting the study parameters and the design parameters, a Groebner basis of the constraint polynomials can be obtained over the ring $\mathbb{C}[h_0, h_1, h_2]$ as a function of Bx_j, By_j and Bz_j, $j = 1, 2, 3$. A graded reverse lexicographic ordering of these variables results in a univariate polynomial of degree eight in any variable Bx_j, By_j or Bz_j. It shows that the inverse kinematics problem of the S–PM at

https://doi.org/10.1017/S0263574718000826 Published online by Cambridge University Press

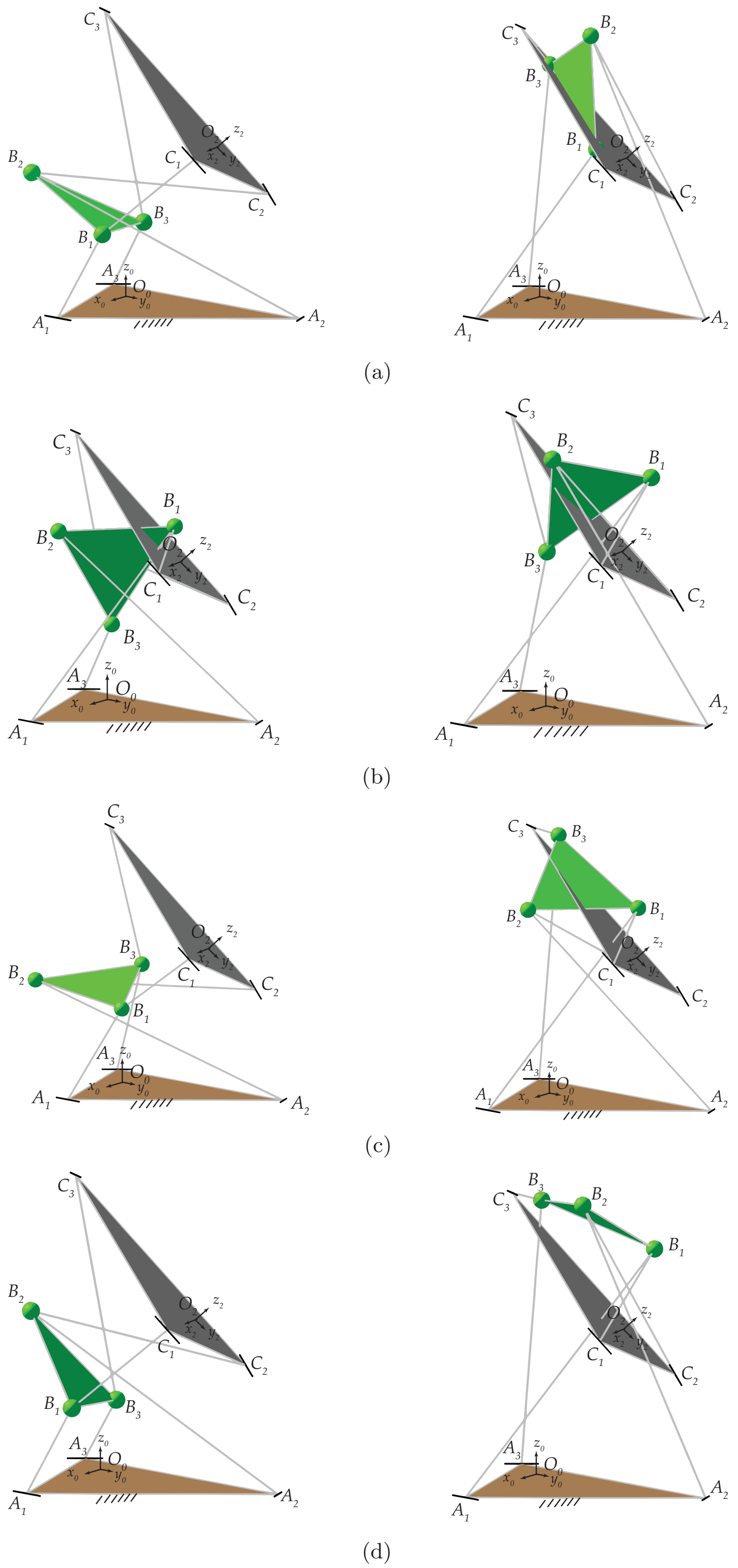

Fig. 8. Eight inverse kinematic solutions for the 3-RPS-3-SPR S–PM when $h_{0=2}$, $h_1 = 1$, $h_{2=2}$ and $(x_0 : x_1 : x_2 : x_3 : y_0 : y_1 : y_2 : y_3) = (2.8215 : -1.2912 : -0.3348 : 1.2434 : 2.1837 : 1.1542 : 1.6012 : -3.3256)$. (a) *Case* a. (b) *Case* b. (c) *Case* c. (d) *Case* d.

https://doi.org/10.1017/S0263574718000826 Published online by Cambridge University Press

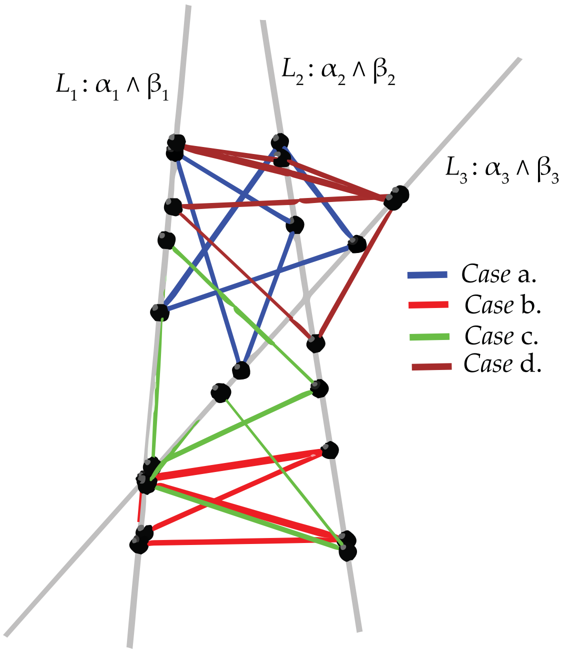

Fig. 9. Eight solutions to IKM as locating three points on three lines problem.

hand has a maximum number of eight solutions. This is not surprising because the problem can be considered as placing three points B_i on three skew lines L_i, $i = 1, 2, 3$, where L_i is the line of intersection of planes α_i and β_i shown in Fig. 1. This is a classical geometrical problem and it has been proven[36] that the maximum number of solutions is indeed eight with a minimal octic univariate polynomial. The interesting feature of the inverse kinematics of the 3-RPS-3-SPR S–PM is that the univariate polynomial factors into four quadratic polynomials. Further examination reveals that the four factors belong to four different combinations of the OM of each module like the four cases shown in Eq. (47). Since the transition between two OM is a constraint singularity, one of the singularities separating the IKM solutions is a constraint singularity[21] in each module.

The IKM is solved for an example with study parameters: $(x_0 : x_1 : x_2 : x_3 : y_0 : y_1 : y_2 : y_3) = (2.8215 : -1.2912 : -0.3348 : 1.2434 : 2.1837 : 1.1542 : 1.6012 : -3.3256)$. The design parameters are chosen to be $h_0 = 2, h_1 = 1, h_2 = 2$. Eight real solutions to IKM are found as shown in Table II.

The corresponding configurations of the S–PM are displayed in Fig. 8. Moreover, the OM of each module is mentioned by recalling the cases from Eq. (47):

- *Case* a. (IKM solutions 1 and 2 in Table II) $c_3 = f_3 = 0 \implies$ 3-RPS$_{\text{OM1}}$ − 3-SPR$_{\text{OM1}}$
- *Case* b. (IKM solutions 3 and 4 in Table II) $c_0 = f_0 = 0 \implies$ 3-RPS$_{\text{OM2}}$ − 3-SPR$_{\text{OM2}}$
- *Case* c. (IKM solutions 5 and 6 in Table II) $c_0 = f_3 = 0 \implies$ 3-RPS$_{\text{OM2}}$ − 3-SPR$_{\text{OM1}}$
- *Case* d. (IKM solutions 7 and 8 in Table II) $c_3 = f_0 = 0 \implies$ 3-RPS$_{\text{OM1}}$ − 3-SPR$_{\text{OM2}}$

There are two inverse kinematic solutions in each of these cases. How these two solutions are separated is still an open issue and is the subject of future work.

Figure 9 presents the eight solutions to the inverse kinematics problem of the manipulator as eight possibilities to locate the three points, B_i on three skew lines $L_i : \alpha_i \wedge \beta_i$, $i = 1, 2, 3$.

7. Conclusions

Study parametrization of individual modules of the 3-RPS-3-SPR S–PM was used to determine six parameters that characterize the manipulator. The kinematic Jacobian matrix was derived and can be used to numerically determine whether a manipulator configuration is singular or not. Moreover, the serial singularities that arise due to the stacking of the two parallel modules were enumerated by mapping these singularities to the degeneracy of the characteristic tetrahedron of the S–PM. Both geometric conditions and algebraic expressions for the serial singularities were established and listed in Table I. The Direct Kinematics Model (DKM) of the 3-RPS-3-SPR S–PM was solved to find out that the maximum number of solutions to the DKM was the product of the maximum number of solutions to the DKM of each module. When each module is restricted to lie in one of the OM, the maximum number of assembly modes is up to 64. Furthermore, the Inverse Kinematics Model (IKM) was solved to find out that the univariate polynomial splits into four factors based on the OM in which each module lies. The number of solutions to the IKM was found to be up to eight and an example was shown to depict those eight solutions.

As a part of the future work, the constraint equations will be written only as a function of input and output parameters in order to solve the DKM directly instead of splitting it into two stages as shown in this paper. Moreover, the workspace of the S–PM will be plotted and the singularities separating the solutions to IKM will be explored.

Acknowledgements

This work was conducted with the support of both Centrale Nantes and the French National Research Agency (ANR project “Kapamat” #ANR-14-CE34-0008-01).

References

1. J. P. Merlet, *Parallel Robots* (Springer Science & Business Media, Netherlands, 2006).
2. L. W. Tsai, *Robot Analysis: The Mechanics of Serial and Parallel Manipulators* (John Wiley & Sons, New York, USA, 1999).
3. T. K. Tanev, “Kinematics of a hybrid (parallelserial) robot manipulator,” *J. Mech. Mach. Theory* **35**(9), 1183–1196 (2000).
4. H. H. Cheng, J. J. Lee and R. Penkar, “Kinematic analysis of a hybrid serial-and-parallel-driven redundant industrial manipulator,” *Int. J. Rob. Aut.* **10**(4), 159–166 (1995).
5. M. Shahinpoor, “Kinematics of a parallel-serial (hybrid) manipulator,” *J. Rob. Syst.* **10**(4), 159–166 (1995).
6. K. J. Waldron, M. Raghavan and B. Roth, “Kinematics of a hybrid series-parallel manipulation system,” *J. Dyn. Sys. Meas. Control* **111**(2), 211–221 (1989).
7. C. Zhang and S.-M. Song, “Geometry and Position Analysis of a Novel Class of Hybrid Manipulators,” *Proceedings of ASME Design Technical Conference* (1994) pp. 1–9.
8. L. Romdhane, “Design and analysis of a hybrid serial-parallel manipulator,” *J. Mech. Mach. Theory* **34**(7), 1037–1055 (1999).
9. X. Z. Zheng, H. Z. Bin and Y. G. Luo, “Kinematic analysis of a hybrid serial-parallel manipulator,” *Int. J. Adv. Manuf. Tech.* **23**(11), 925–930 (2004).
10. B. Hu, J. Yu, Y. Lu, C. Sui and J.Han, “Statics and stiffness model of serial-parallel manipulator formed by k parallel manipulators connected in series,” *ASME. J. Mech. Rob.* **4**(2), pp. 021012–021012–8 (2012).
11. Y. Lu and B. Hu, “Analysis of kinematics/statics and workspace of a 2(SP+SPR+SPU) serial–parallel manipulator,” *J. Multibody Syst. Dyn.* **21**(4), 361–70 (1999).
12. J. G. Alvarado, C. R. A. Njera, L. C. Rosas, J. M. R. Martnez and M. N. Islam, “Kinematics and dynamics of 2(3-RPS) manipulators by means of screw theory and the principle of virtual work,” *J. Mech. Mach. Theory* **43**(10), 1281–1294 (2008).
13. B. Hu, L. Yi, J. J. Yu and S. Zhuang, “Analyses of Inverse Kinematics, Statics and Workspace of a Novel 3-RPS-3-SPR Serial-Parallel Manipulator,” *J. Mech. Eng.* **M1**(6), 65–72 (2012).
14. B. Hu, “Formulation of unified Jacobian for serial-parallel manipulators,” *Robotics and Computer-Integr. Manuf.* **30**(5), 460–467 (2014).
15. J. G. -Alvarado, L. P. -González, G. R. Mondragón, H. R. Garduño and A. T. Villagómez, “Mobility and Velocity Analysis of a Limited-dof Series-Parallel Manipulator,” *Conference: XVII COMRob 2015, Mexican Robotics Congress* (2015)
16. K. H. Hunt, *Kinematic Geometry of Mechanisms* (Oxford University Press, Oxford, UK, c. 1978).
17. A. Nayak, S. Caro and P. Wenger, “Local and Full-Cycle Mobility Analysis of a 3-RPS-3-SPR Series-Parallel Manipulator,” *Proceedings of the 7th International Workshop on Computational Kinematics* (2018) pp. 499–507.
18. M. L. Husty, M. Pfurner, H. P. Schröcker and K. Brunnthaler, “Algebraic methods in mechanism analysis and synthesis,” *J. Robotica* **25**(6), 661–675 (2007).
19. M. L. Husty and H. P. Schröcker, “Kinematics and Algebraic Geometry,” *Proceedings of the 21st Century Kinematics* (2013) pp. 85–123.
20. T. Stigger and M. L. Husty, “Constraint Equations of Inverted Kinematic Chains,” *Proceedings of the 7th International Workshop on Computational Kinematics* (2018) pp. 491–498.
21. J. Schadlbauer, D. R. Walter and M. L. Husty, “The 3-RPS parallel manipulator from an algebraic viewpoint,” *J. Mech. Mach. Theory* **75**, 161–176 (2014).
22. I. Ebert-Uphoff, J. K. Lee and H. Lipkin, “Characteristic tetrahedron of wrench singularities for parallel manipulators with three legs,” *Proc. Inst Mech. Eng., Part C: J. Mech. Eng. Sci.* **216**(1), 81–93 (2002).

23. S. A. Joshi and L. W. Tsai, "Jacobian analysis of limited-DOF parallel manipulators," *ASME J. Mech. Des.* **124**(2), 254–258 (2002).
24. A. Nayak, L. Nurhami, P. Wenger and S. Caro, "Comparison of 3-RPS and 3-SPR Parallel Manipulators Based on Their Maximum Inscribed Singularity-Free Circle," *New Trends in Mechanism and Machine Science* (2017) pp. 121–130.
25. R. Kalla, L. Nurhami, S. Bandyopadhay, P. Wenger and S. Caro, "A Study of Σ2 Singularities in the 3-RPS Parallel Manipulator," *Proceedings of the 2nd International and 17th National Conference on Machines and Mechanisms,* India (2015).
26. J. Schadlbauer, M. L. Husty, S. Caro and P.Wenger, "Self-motions of 3-RPS manipulators," *ASME J. Frontiers Mech. Eng.* **8**(1), 62–69 (2013).
27. S. Amine, O. Mokhiamar and S. Caro, "Classification of 3T1R parallel manipulators based on their wrench graph," *ASME. J. Mech. Rob.* **9**(1), 011003-011003-10 (2017).
28. S. Amine, S. Caro, P. Wenger and D. Kanaan, "Singularity analysis of the H4 robot using Grassmann Cayley algebra," *J. Robotica* **9**(1), 1109–1118 (2012).
29. S. Amine, M. T. Masouleh, S. Caro, P. Wenger and C.Gosselin, "Singularity conditions of 3T1R parallel manipulators with identical limb structures," *ASME. J. Mech. Rob.* **4**(1), 011011-1 011011-11 (2012).
30. S. Maraje, L. Nurhami and S. Caro, "Operation Modes Comparison of a Reconfigurable 3-PRS Parallel Manipulator Based on Kinematic Performance," *Proceedings of the ASME 2016 International Design Engineering Technical Conferences and Computers and Information in Engineering Conference, IDETC/CIE 2016*, Charlotte, North Carolina, USA, Aug. 21–24 (2016).
31. S. Caro, G. Moroz, T. Gayral, D. Chablat and C. Chen, "Singularity Analysis of a Six-dof Parallel Manipulator using Grassmann–Cayley Algebra and Groebner Bases," *Symposium on Brain, Body and Machine*, Montreal, QC, Canada, November 10–12. (2010) pp. 341–352.
32. J. P. Merlet, "Singular Configurations of Parallel Manipulators and Grassmann Geometry," *Geometry and Robotics: Workshop, Toulouse, France* (1989) pp. 194–212.
33. H. Pottmann and J. Wallner, *Computational Line Geometry* (Springer-Verlag New York, Inc., 2001).
34. I. A. Bonev, D. Zlatanov and C. M. Gosselin, "Advantages of the Modified Euler Angles in the Design and Control of PKMs," *Proceedings of the Parallel Kinematic Machines International Conference* (2002) pp. 171–188.
35. E. A. Weiss, *Einführung in Die Liniengeometrie und Kinematik* (B. G. Teubner, Leibzig, 1935).
36. J. C. F. Shum, and P. J. Zsombor-Murray, "Direct Kinematics of the Double-Triangular Manipulator: An Exercise in Geometric Thinking." **In:** *Advances in Robot Kinematics.* (J. Lenarčič and M. M. Stanišić eds.) (Springer, Dordrecht, 2000).

Appendix

Direct kinematics: Translational parameters, y_i, $i = 0, 1, 2, 3$ as functions of $f_1, f_2, g_1, c_1, c_2, d_1$.

$$
\begin{aligned}
y_0 = {} & \frac{1}{2\left(f_1^2+f_2^2+1\right)\left(c_1^2+c_2^2+1\right)c_2f_2}(2\,c_1^3c_2f_1^2f_2g_1+c_1^3c_2f_1^2f_2h_1+2\,c_1^3c_2f_2^3g_1 \\
& +c_1^3c_2f_2^3h_1-2\,c_1^3d_1f_1^2f_2^2-2\,c_1^3d_1f_2^4+c_1^3f_1^2f_2^2h_1+c_1^3f_2^4h_1-2\,c_1^2c_2^2f_1^3g_1 \\
& -c_1^2c_2^2f_1^3h_1-2\,c_1^2c_2^2f_1f_2^2g_1+3\,c_1^2c_2^2f_1f_2^2h_1+2\,c_1^2c_2d_1f_1^3f_2+2\,c_1^2c_2d_1f_1f_2^3 \\
& -c_1^2c_2f_1^3f_2h_1+3\,c_1^2c_2f_1f_2^3h_1+2\,c_1c_2^3f_1^2f_2g_1-3\,c_1c_2^3f_1^2f_2h_1+2\,c_1c_2^3f_2^3g_1 \\
& -3\,c_1c_2^3f_2^3h_1-2\,c_1c_2^2d_1f_1^2f_2^2-2\,c_1c_2^2d_1f_2^4-3\,c_1c_2^2f_1^2f_2^2h_1-3\,c_1c_2^2f_2^4h_1 \\
& -2\,c_2^4f_1^3g_1-c_2^4f_1^3h_1-2\,c_2^4f_1f_2^2g_1+3\,c_2^4f_1f_2^2h_1+2\,c_2^3d_1f_1^3f_2+2\,c_2^3d_1f_1f_2^3 \\
& -c_2^3f_1^3f_2h_1+3\,c_2^3f_1f_2^3h_1+2\,c_1^3c_2f_2g_1+c_1^3c_2f_2h_1-2\,c_1^3d_1f_2^2+c_1^3f_2^2h_1 \\
& -2\,c_1^2c_2^2f_1g_1+2\,c_1^2c_2d_1f_1f_2+2\,c_1c_2^3f_2g_1-3\,c_1c_2^3f_2h_1-2\,c_1c_2^2d_1f_2^2-3\,c_1c_2^2f_2^2h_1 \\
& +2\,c_1c_2f_1^2f_2g_1+2\,c_1c_2f_2^3g_1-2\,c_1d_1f_1^2f_2^2-2\,c_1d_1f_2^4-2\,c_2^4f_1g_1+2\,c_2^3d_1f_1f_2 \\
& -2\,c_2^2f_1^3g_1-c_2^2f_1^3h_1-2\,c_2^2f_1f_2^2g_1+3\,c_2^2f_1f_2^2h_1+2\,c_2d_1f_1^3f_2+2\,c_2d_1f_1f_2^3 \\
& -c_2f_1^3f_2h_1+3\,c_2f_1f_2^3h_1+2\,c_1c_2f_2g_1-2\,c_1d_1f_2^2-2\,c_2^2f_1g_1+2\,c_2d_1f_1f_2)
\end{aligned}
\tag{A1}
$$

$$
\begin{aligned}
y_1 = {} & \frac{1}{2\left(f_1^2+f_2^2+1\right)\left(c_1^2+c_2^2+1\right)c_2f_2}(4\,c_1^3c_2f_1f_2^3h_1+4\,c_1^2c_2^2f_2^4h_1-4\,c_1c_2^3f_1^3f_2h_1 \\
& -4\,c_2^4f_1^2f_2^2h_1+c_1^3c_2f_1f_2h_1-2\,c_1^2c_2^2f_1^2g_1-c_1^2c_2^2f_1^2h_1-2\,c_1^2c_2^2f_2^2g_1
\end{aligned}
$$

https://doi.org/10.1017/S0263574718000826 Published online by Cambridge University Press

$$+ 4\,c_1{}^2c_2{}^2f_2{}^2h_1 - 2\,c_1{}^2c_2d_1f_1{}^2f_2 - 2\,c_1{}^2c_2d_1f_2{}^3 - 2\,c_1{}^2c_2f_1{}^2f_2g_1 - 2\,c_1{}^2c_2f_2{}^3g_1$$
$$- 2\,c_1{}^2d_1f_1{}^2f_2{}^2 - 2\,c_1{}^2d_1f_2{}^4 + c_1{}^2f_1{}^2f_2{}^2h_1 + c_1{}^2f_2{}^4h_1 - 3\,c_1c_2{}^3f_1f_2h_1 - c_1c_2f_1{}^3f_2h_1$$
$$+ 3\,c_1c_2f_1f_2{}^3h_1 - 2\,c_2{}^4f_1{}^2g_1 - c_2{}^4f_1{}^2h_1 - 2\,c_2{}^4f_2{}^2g_1 - 2\,c_2{}^3d_1f_1{}^2f_2 - 2\,c_2{}^3d_1f_2{}^3$$
$$- 2\,c_2{}^3f_1{}^2f_2g_1 - 2\,c_2{}^3f_2{}^3g_1 - 2\,c_2{}^2d_1f_1{}^2f_2{}^2 - 2\,c_2{}^2d_1f_2{}^4 - 4\,c_2{}^2f_1{}^2f_2{}^2h_1 - 2\,c_1{}^2c_2{}^2g_1$$
$$- 2\,c_1{}^2c_2d_1f_2 - 2\,c_1{}^2c_2f_2g_1 - 2\,c_1{}^2d_1f_2{}^2 + c_1{}^2f_2{}^2h_1 - 2\,c_2{}^4g_1 - 2\,c_2{}^3d_1f_2 - 2\,c_2{}^3f_2g_1$$
$$- 2\,c_2{}^2d_1f_2{}^2 - 2\,c_2{}^2f_1{}^2g_1 - c_2{}^2f_1{}^2h_1 - 2\,c_2{}^2f_2{}^2g_1 - 2\,c_2d_1f_1{}^2f_2 - 2\,c_2d_1f_2{}^3 - 2\,c_2f_1{}^2f_2g_1$$
$$- 2\,c_2f_2{}^3g_1 - 2\,d_1f_1{}^2f_2{}^2 - 2\,d_1f_2{}^4 - 2\,c_2{}^2g_1 - 2\,c_2d_1f_2 - 2\,c_2f_2g_1 - 2\,d_1f_2{}^2) \qquad \text{(A2)}$$

$$y_2 = \frac{1}{2\left(f_1{}^2+f_2{}^2+1\right)\left(c_1{}^2+c_2{}^2+1\right)c_2f_2}(4\,c_1{}^3c_2f_1{}^2f_2{}^2h_1 - 4\,c_1{}^2c_2{}^2f_1{}^3f_2h_1 - 4\,c_1c_2{}^3f_2{}^4h_1$$
$$+ 4\,c_2{}^4f_1f_2{}^3h_1 + 2\,c_1{}^3c_2f_1{}^2g_1 + c_1{}^3c_2f_1{}^2h_1 + 2\,c_1{}^3c_2f_2{}^2g_1 + 2\,c_1{}^3d_1f_1{}^2f_2 + 2\,c_1{}^3d_1f_2{}^3$$
$$- c_1{}^3f_1{}^2f_2h_1 - c_1{}^3f_2{}^3h_1 - 3\,c_1{}^2c_2{}^2f_1f_2h_1 + 2\,c_1{}^2c_2f_1{}^3g_1 + c_1{}^2c_2f_1{}^3h_1 + 2\,c_1{}^2c_2f_1f_2{}^2g_1$$
$$- 3\,c_1{}^2c_2f_1f_2{}^2h_1 + 2\,c_1{}^2d_1f_1{}^3f_2 + 2\,c_1{}^2d_1f_1f_2{}^3 - c_1{}^2f_1{}^3f_2h_1 - c_1{}^2f_1f_2{}^3h_1 + 2\,c_1c_2{}^3f_1{}^2g_1$$
$$+ c_1c_2{}^3f_1{}^2h_1 + 2\,c_1c_2{}^3f_2{}^2g_1 - 4\,c_1c_2{}^3f_2{}^2h_1 + 2\,c_1c_2{}^2d_1f_1{}^2f_2 + 2\,c_1c_2{}^2d_1f_2{}^3$$
$$+ 3\,c_1c_2{}^2f_1{}^2f_2h_1 + 3\,c_1c_2{}^2f_2{}^3h_1 + 3\,c_1c_2f_1{}^2f_2{}^2h_1 - c_1c_2f_2{}^4h_1 + c_2{}^4f_1f_2h_1 + 2\,c_2{}^3f_1{}^3g_1$$
$$+ c_2{}^3f_1{}^3h_1 + 2\,c_2{}^3f_1f_2{}^2g_1 - 3\,c_2{}^3f_1f_2{}^2h_1 + 2\,c_2{}^2d_1f_1{}^3f_2 + 2\,c_2{}^2d_1f_1f_2{}^3 + 4\,c_2{}^2f_1f_2{}^3h_1$$
$$+ 2\,c_1{}^3c_2g_1 + 2\,c_1{}^3d_1f_2 - c_1{}^3f_2h_1 + 2\,c_1{}^2c_2f_1g_1 + 2\,c_1{}^2d_1f_1f_2 - c_1{}^2f_1f_2h_1 + 2\,c_1c_2{}^3g_1$$
$$+ 2\,c_1c_2{}^2d_1f_2 + 3\,c_1c_2{}^2f_2h_1 + 2\,c_1c_2f_1{}^2g_1 + c_1c_2f_1{}^2h_1 + 2\,c_1c_2f_2{}^2g_1 - c_1c_2f_2{}^2h_1$$
$$+ 2\,c_1d_1f_1{}^2f_2 + 2\,c_1d_1f_2{}^3 + 2\,c_2{}^3f_1g_1 + 2\,c_2{}^2d_1f_1f_2 + c_2{}^2f_1f_2h_1 + 2\,c_2f_1{}^3g_1 + c_2f_1{}^3h_1$$
$$+ 2\,c_2f_1f_2{}^2g_1 - 3\,c_2f_1f_2{}^2h_1 + 2\,d_1f_1{}^3f_2 + 2\,d_1f_1f_2{}^3 + 2\,c_1c_2g_1 + 2\,c_1d_1f_2 + 2\,c_2f_1g_1$$
$$+ 2\,d_1f_1f_2) \qquad \text{(A3)}$$

$$y_3 = \frac{1}{2\left(f_1{}^2+f_2{}^2+1\right)\left(c_1{}^2+c_2{}^2+1\right)c_2f_2}(2\,c_1{}^3c_2f_1{}^3g_1 + c_1{}^3c_2f_1{}^3h_1 + 2\,c_1{}^3c_2f_1f_2{}^2g_1$$
$$- 3\,c_1{}^3c_2f_1f_2{}^2h_1 - 2\,c_1{}^3d_1f_1{}^3f_2 - 2\,c_1{}^3d_1f_1f_2{}^3 + c_1{}^3f_1{}^3f_2h_1 + c_1{}^3f_1f_2{}^3h_1$$
$$+ 2\,c_1{}^2c_2{}^2f_1{}^2f_2g_1 - 3\,c_1{}^2c_2{}^2f_1{}^2f_2h_1 + 2\,c_1{}^2c_2{}^2f_2{}^3g_1 - 3\,c_1{}^2c_2{}^2f_2{}^3h_1 - 2\,c_1{}^2c_2d_1f_1{}^2f_2{}^2$$
$$- 2\,c_1{}^2c_2d_1f_2{}^4 - 3\,c_1{}^2c_2f_1{}^2f_2{}^2h_1 + c_1{}^2c_2f_2{}^4h_1 + 2\,c_1c_2{}^3f_1{}^3g_1 + c_1c_2{}^3f_1{}^3h_1$$
$$+ 2\,c_1c_2{}^3f_1f_2{}^2g_1 - 3\,c_1c_2{}^3f_1f_2{}^2h_1 - 2\,c_1c_2{}^2d_1f_1{}^3f_2 - 2\,c_1c_2{}^2d_1f_1f_2{}^3 - 3\,c_1c_2{}^2f_1{}^3f_2h_1$$
$$- 3\,c_1c_2{}^2f_1f_2{}^3h_1 + 2\,c_2{}^4f_1{}^2f_2g_1 + c_2{}^4f_1{}^2f_2h_1 + 2\,c_2{}^4f_2{}^3g_1 + c_2{}^4f_2{}^3h_1 - 2\,c_2{}^3d_1f_1{}^2f_2{}^2$$
$$- 2\,c_2{}^3d_1f_2{}^4 - 3\,c_2{}^3f_1{}^2f_2{}^2h_1 + c_2{}^3f_2{}^4h_1 + 2\,c_1{}^3c_2f_1g_1 - 2\,c_1{}^3d_1f_1f_2 + c_1{}^3f_1f_2h_1$$
$$+ 2\,c_1{}^2c_2{}^2f_2g_1 - 3\,c_1{}^2c_2{}^2f_2h_1 - 2\,c_1{}^2c_2d_1f_2{}^2 - 2\,c_1{}^2c_2f_1{}^2g_1 - c_1{}^2c_2f_1{}^2h_1 - 2\,c_1{}^2c_2f_2{}^2g_1$$
$$+ c_1{}^2c_2f_2{}^2h_1 + 2\,c_1{}^2d_1f_1{}^2f_2 + 2\,c_1{}^2d_1f_2{}^3 - c_1{}^2f_1{}^2f_2h_1 - c_1{}^2f_2{}^3h_1 + 2\,c_1c_2{}^3f_1g_1$$
$$- 2\,c_1c_2{}^2d_1f_1f_2 - 3\,c_1c_2{}^2f_1f_2h_1 + 2\,c_1c_2f_1{}^3g_1 + c_1c_2f_1{}^3h_1 + 2\,c_1c_2f_1f_2{}^2g_1$$
$$- 3\,c_1c_2f_1f_2{}^2h_1 - 2\,c_1d_1f_1{}^3f_2 - 2\,c_1d_1f_1f_2{}^3 + 2\,c_2{}^4f_2g_1 + c_2{}^4f_2h_1 - 2\,c_2{}^3d_1f_2{}^2$$
$$- 2\,c_2{}^3f_1{}^2g_1 - c_2{}^3f_1{}^2h_1 - 2\,c_2{}^3f_2{}^2g_1 + c_2{}^3f_2{}^2h_1 + 2\,c_2{}^2d_1f_1{}^2f_2 + 2\,c_2{}^2d_1f_2{}^3$$

https://doi.org/10.1017/S0263574718000826 Published online by Cambridge University Press

$$+ 2\,c_2{}^2 f_1{}^2 f_2 g_1 + c_2{}^2 f_1{}^2 f_2 h_1 + 2\,c_2{}^2 f_2{}^3 g_1 + c_2{}^2 f_2{}^3 h_1 - 2\,c_2 d_1 f_1{}^2 f_2{}^2 - 2\,c_2 d_1 f_2{}^4$$
$$- 3\,c_2 f_1{}^2 f_2{}^2 h_1 + c_2 f_2{}^4 h_1 - 2\,c_1{}^2 c_2 g_1 + 2\,c_1{}^2 d_1 f_2 - c_1{}^2 f_2 h_1 + 2\,c_1 c_2 f_1 g_1 - 2\,c_1 d_1 f_1 f_2$$
$$- 2\,c_2{}^3 g_1 + 2\,c_2{}^2 d_1 f_2 + 2\,c_2{}^2 f_2 g_1 + c_2{}^2 f_2 h_1 - 2\,c_2 d_1 f_2{}^2 - 2\,c_2 f_1{}^2 g_1 - c_2 f_1{}^2 h_1 - 2\,c_2 f_2{}^2 g_1$$
$$+ c_2 f_2{}^2 h_1 + 2\,d_1 f_1{}^2 f_2 + 2\,d_1 f_2{}^3 - 2\,c_2 g_1 + 2\,d_1 f_2) \tag{A4}$$

https://doi.org/10.1017/S0263574718000826 Published online by Cambridge University Press